Received: 10 October 2014
IOTC–2014–WPEB10–34

PRELIMINARY REPORT

Indian Ocean Tuna Commission

Marine Ecosystem Department
Space Oceanography Division
CLS
8-10 rue Hermès
31520, Ramonville, France

October 2014

Written by:
AC. Dragon, I. Senina, P. Lehodey

Copy to:
IOTC: J. Bourjea, D. Wilson
CLS: P. Lehodey, I Senina, AC. Dragon, P. Gaspar, G. Larnicol, S Limouzin

Applications of the SEAPODYM model to swordfish in the Pacific and Indian Oceans

Abstract:

In 2011, a first Spatial Ecosystem And Population Dynamic Model (SEAPODYM) application to Pacific swordfish (*Xiphias gladius*) was developed in collaboration with the Secretariat of the Pacific Community (SPC) and the PIFSC/NOAA (Hawaii, USA). The objective was to investigate the impacts of both fishing and climate variability on this species. The oceanic environment used to force SEAPODYM was predicted from a coupled physical-biogeochemical ocean model (NEMO-PISCES) driven by an atmospheric reanalysis (NCEP) on a 2° x month resolution (ORCA2 grid) over the historical fishing period (1948-2003). Available spatially-disaggregated catch per unit of effort (CPUE) and length-frequency data from the fisheries operating in the Pacific Ocean were assimilated into the model to achieve parameter optimization with a Maximum Likelihood Estimation (MLE) approach. The preliminary results suggested the existence of 3 overlapping adult core habitats, in good agreement with previous hypotheses of 3 sub-stocks mentioned in the literature (Kolody et al. 2009; Hinton & Maunder 2011; Courtney and Piner 2009), but nevertheless linked by their common tropical spawning grounds.

This Pacific-based optimal parameterization has been used to develop a SEAPODYM model configuration to the Indian swordfish population. Simulations are driven by 1952-2012 historical geo-referenced catch data and by the same environmental forcing (NCEP-ORCA2). The MLE approach based on fisheries data was used here only to estimate fisheries catchability. Preliminary selectivities of fishing gears were fixed. The fisheries defined for the Indian Ocean swordfish represent 90% of the pelagic longline catches in the Indian Ocean, though in average 80% of this catch is provided under a geo-referenced form. The analysis of spatially disaggregated catch and effort data shows several major fishing grounds with one core region in the Southwest sector of the Indian Ocean. A series of simulations was conducted to determine the minimum swordfish biomass required to fit correctly at least 95% of spatially disaggregated catch data.

This first application, with minor changes in the optimization of habitats and population dynamics parameters achieved in the Pacific Ocean, was validated with catch and effort data. These preliminary results indicate that the proposed solution is already reasonably coherent with many features that characterize the swordfish population dynamics and fisheries in the Indian Ocean. A fully optimized configuration of the model should be therefore achievable in a reasonable timeframe. Once the optimal solution will be completed, the model could be used to estimate an average maximum sustainable yield accounting for interannual and decadal variability. Given its spatial structure, it can serve to investigate the connectivity of the stock(s) between any oceanic regions or EEZs. Finally, projections of population trends under different IPCC scenarios of Climate Change could be tested to compute possible change in MSY for the coming decades, and a Indo-Pacific configuration envisaged to increase the fishing dataset and the diversity of environmental conditions used with the MLE framework.

1 Forewords

The Spatial Ecosystem And Population Dynamics Model (SEAPODYM) is developed for investigating spatial population dynamics of fish and tuna particularly, under the influence of both fishing and environmental effects. The model is based on advection-diffusion-reaction equations. Population dynamics (spawning, movement, mortality) are constrained by environmental data (temperature, currents, primary production and dissolved oxygen concentration) and simulated distribution of mid-trophic (micronektonic tuna forage) functional groups. Different life stages are considered: larvae, juveniles and (immature and mature) adults. After juvenile phase, fish become autonomous, i.e., they have their own movement (linked to their size and habitat) in addition to be transported by oceanic currents. The model includes a representation of fisheries and predicts total catch and size frequency of catch by fleet when fishing data (catch and effort) are available. A Maximum Likelihood Estimation (MLE) approach is used to optimize the model parameters. Conventional tagging larvae density and acoustic biomass estimates data have been added recently in the MLE approach (Senina et al. 2008).

In addition to the tuna population dynamics, temperature and currents variables are also used in the model to predict the forage biomass distributions (Lehodey et al. 2010a). Forage gathers potential prey for young and adult tunas and the predators of their larvae. However, the parameters of the forage model have been calibrated and described in a separate study (Lehodey et al. 2010a). Applications of SEAPODYM to Pacific tuna and swordfish have been extensively described in the scientific literature (Senina et al. 2008; Lehodey et al. 2010b; Sibert et al. 2012; Lehodey et al. 2013a). The continuous development and progress with this model and applications to Pacific tuna stocks are reported to the WCPFC Scientific Committee and is facilitated through the Project 62 (Lehodey et al. 2013b). The model is also currently applied to the Atlantic albacore and South Pacific Jack Mackerel and a regional operational application is being implemented for the Indonesian government for the monitoring and management of Indonesian skipjack, yellowfin and bigeye tuna fisheries.

2 First SEAPODYM application to Indian swordfish

The Pacific-based optimal parameterization of SEAPODYM for swordfish (see appendix) has been used to obtain a configuration for the Indian swordfish population. Simulations are driven by 1952-2012 historical geo-referenced catch data (Figure 1) and by the same environmental forcing (NCEP-ORCA2). Available catch per unit of effort (CPUE) data from the fisheries operating in the study area were used with the MLE approach to estimate fisheries catchability parameters.

2.1 Fishing data

Globally, swordfish is one of the most widely distributed pelagic fish species and represents an important fishery resource in the entire Indian Ocean. Distributions of catch and effort data in the Indian Ocean show several major fishing grounds with two core regions respectively in the Southwest and Northwest sectors (Fig. 1).

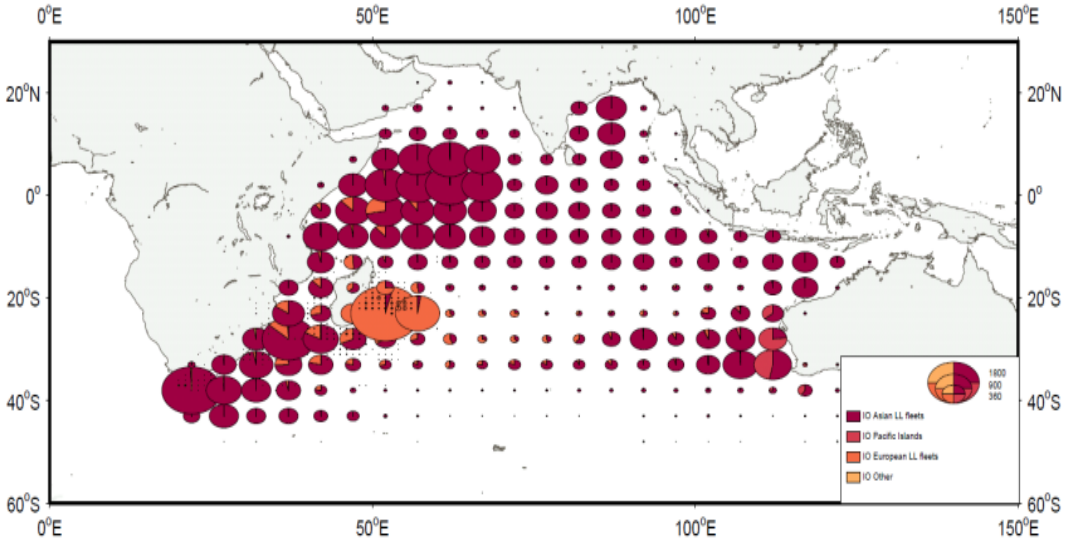

Figure 1: Total swordfish catch from 1952-2012. "IO Asian LL fleets" gathers Taiwan, Japan and Korea fleets."IO Pacific Islands" stands for Australia. "IO European LL fleets" regroups Spanish and French fleets. "IO other" stands for the South African fleet. Data source: IOTC.

Swordfish catch in the Indian Ocean are reported by twenty different Countries at the Indian Ocean Tuna Commission (IOTC). The annual catch started to quickly increase after 1990, to reach a maximum range of 35 000 – 40 000 metric tonnes (mt) between 1998 and 2003. Since then, the total declared annual catch has decreased and stabilized to 25 000 mt over the last 5 years (Fig. 2)

Data gathered on the life history of this species is scarce and patchy despite the growing scientific interest for swordfish in the Indian Ocean. Several scientific national or multilateral programs focusing on swordfish fisheries have been undertaken during the last decade (IOTC, 2007). However, most of the studies are conducted in limited geographical areas (especially in the western Indian Ocean). To our knowledge, no comprehensive study of swordfish reproduction dynamics has been carried out over the entire Indian Ocean.

The status of the stock(s) is also unclear. On the basis of stock indicators, the IOTC Scientific Committee concluded in 2008 that the current level of catch at that time (about 32 000 t) was unlikely to be sustainable (Poisson & Fauvel 2009). The committee also highlighted that swordfish life history

characteristics, i.e., high age-at-maturity, long lifespan and sexual dimorphism, make this species particularly vulnerable to overexploitation (IOTC, 2007).

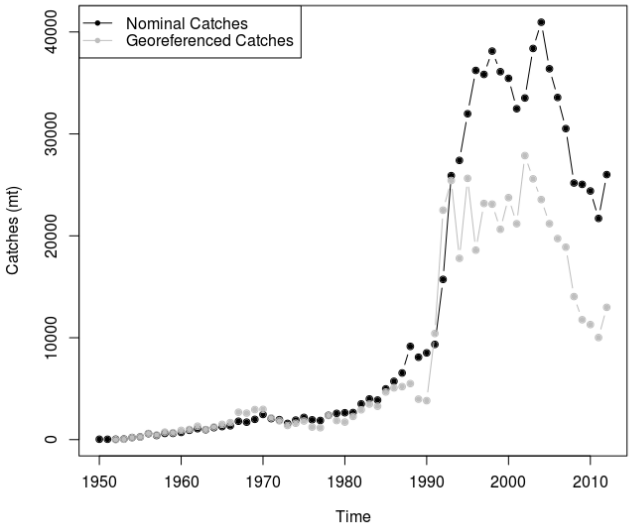

Figure 2: Time series of annual catch data with geographical coordinates used in the simulation with SEAPODYM and total annual catch declared to IOTC for the Indian swordfish fisheries over the historical fishing period. When data were declared in number of fish, a conversion factor has been used, i.e., 61 kg fish−1.

For this study covering the entire Indian Ocean basin, the fishing data sets available were geo-referenced catch and effort data provided by IOTC. No length-frequency data were available yet to be assimilated into the model. Table 1 summarizes the fishing data included in this analysis. The fisheries defined for the Indian Ocean swordfish represent 90% of the pelagic longline catches in the Indian Ocean, though in average 80% of this catch is provided under a geo-referenced form (Figure 1).

Fishing data provided by IOTC for most longline fisheries were at the resolution of the model (2ºx2ºx month). Until the end of the 1980s the catch of Pacific swordfish was essentially due to the Asian longliners (Fig. 3, especially Japan). Then several other longline fisheries progressively increased their fishing effort and catch of swordfish either as a target species or bycatch, while conversely the Asian longline catch decreased.

Table 1. Main fisheries definition for the Indian swordfish.

ID	Gear	Region	Description	Nationality	units	available catch/effort	Resolution
L1	LL	20°-70°E 40°S-20°S	pooled LL targeting swordfish	South Africa	mt	1998-2012	2°x2°
L2	LL	95°-140°E 40°S-10°S	pooled LL targeting swordfish	Australia	mt	1992-2012	2°x2°
L3	LL	95°-140°E 40°S-10°S	pooled LL targeting swordfish	Australia	Nb fish	1992-2000	2°x2°
L4	LL	20°-120°E 50°S-20°N	pooled LL	Korea	mt	1994-2012	2°x2°
L5	LL	20°-120°E 50°S-20°N	pooled LL	Korea	Nb fish	1974-2012	2°x2°

L6	LL	20°-110°E 40°S-10°N	pooled LL targeting swordfish	Spain	mt	1994-2012	2°x2°
L7	LL	30°-60°E 40°S-10°S	pooled LL targeting swordfish	France-La Réunion	mt	2001-2012	0.5°x0.5°
L8	LL	30°-60°E 35°S-5°N	pooled LL targeting swordfish	France-La Réunion	Nb fish	1994-2001	2°x2°
L9	LL	20°-150°E 50°S-20°N	pooled LL	Japan	Nb fish	1952-2012	2°x2°
L10	LL	20°-150°E 50°S-20°N	pooled LL	Taiwan	mt	1967-1991	2°x2°
L11	LL	20°-150°E 50°S-20°N	pooled LL	Taiwan	mt	1992-2012	2°x2°

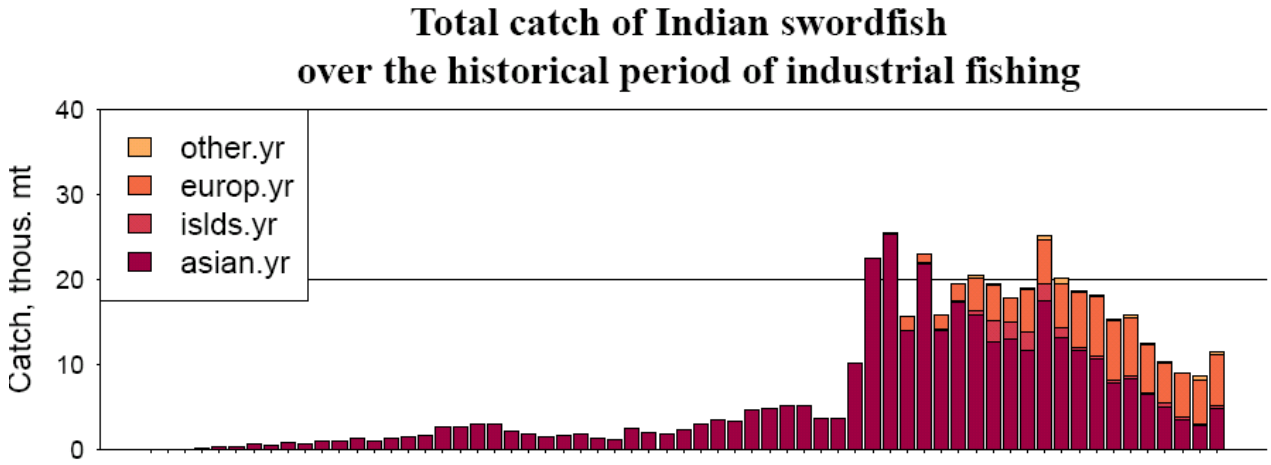

Figure 3: Swordfish annual catch by flag. Data provided by IOTC for the whole Indian Ocean for the main contributors to the swordfish fisheries. "IO Asian LL fleets" gathers Taiwan, Japan and Korea fleets."IO Pacific Islands" stands for Australia. "IO European LL fleets" regroups Spanish and French fleets. "IO other" stands for the South African fleet.

2.2 Optimization experiments

For this first application of SEAPODYM to the Indian basin, we did not change the optimal parameterization achieved in the Pacific Ocean for habitats, mortality, movements, and population dynamics. The MLE approach however was used with the geo-referenced fishing data over the period 1980-2003 to estimate fisheries catchability. Preliminary selectivity functions of fishing gears were fixed. Based on observed fishing effort, the predicted catches were aggregated or redistributed at the resolution of the data (2° x month) before contributing to the likelihood. The optimal solution is thus based on unchanged Pacific parameterization except for the catchability of Indian Ocean swordfish fisheries.

2.3 Population structure

The model simulates age-structured swordfish populations with one length and one weight coefficient per age cohort (males and females combined) obtained from independent studies (see appendix). Globally, the population structure for the experiment in the Indian Ocean (Figure 4) was very similar

to the one in the Pacific except for (i) a pound-to-kilo correction applied to the vector of weight at age and (ii) a monthly age structure with 108 monthly cohorts and one A+ cohort.

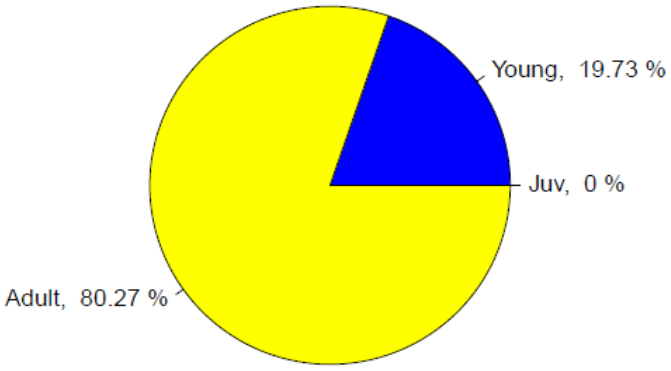

Figure 4. Age structure used in the swordfish configuration and estimated stage composition in metric tones by life stage. (Note that the 0% for juvenile is due to the rounding of values because it is less than 0.01% in weight)

2.4 Fit to catch data

The overall spatial coverage of effort and catch data encompasses all the Indian Ocean between 45°S and 20°N (Fig. 5). Except for a few exceptions, the poorly fitted areas correspond to areas of low levels of catch, outside of the main swordfish fishing grounds described above from Fig 1. The variance is relatively well explained by the model and relative error on predicted catch significant only in cells of very weak catch and effort (Fig 5). Around La Réunion Island, the fit is particularly high with the fishing data that were provided at the resolution of the model grid, highlighting the importance of a good accuracy in fishing data. Beside, the French longline fisheries at La Réunion Island (L7 and L8) get very high correlation ($r > 0.95$) over time for catch and CPUE (Fig. 6). The fisheries L4, L5, L10 and L11 targeting tuna species (cf. Table 1) get high correlations ($r > 0.8$) over time. The fit between predicted and observed catch and CPUE still remain good for other fisheries except Japan (L9). For this latter fishery, it would be useful to access to a better definition of target species and fishing strategy (e.g., deep or shallow sets). Globally, the fit achieved for the fisheries is high but could be likely improved with a better selectivity parameterization using size frequency data.

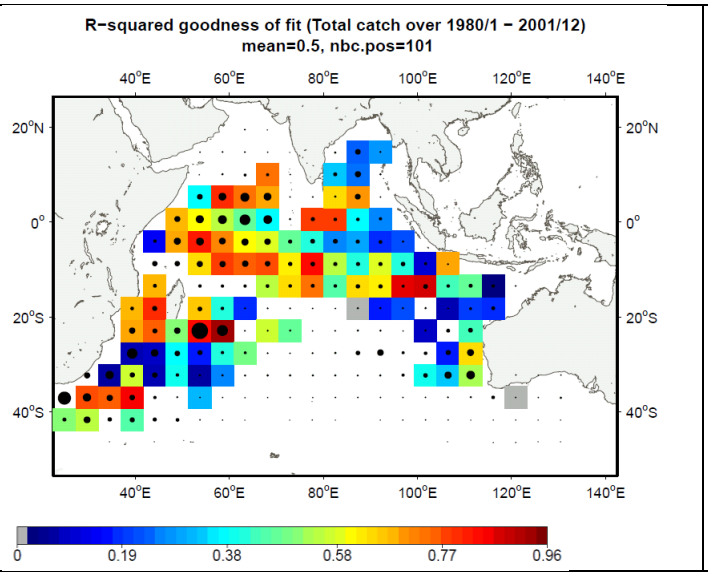

Figure 5. Spatial fit to catch data.

Top: Map of R-squared goodness of fit metrics representing the spatial fit over the period used for optimization (white squares indicate negative correlation between observations and predictions), overlaid with the total catch in each cell (black circles proportional to catch)

.

Middle: Map of Pearson r-squared metric, which quantifies the percentage of the catch variance explained by the model in each cell, overlaid with the number of observations (fishing events).

Bottom: Map of the mean error.

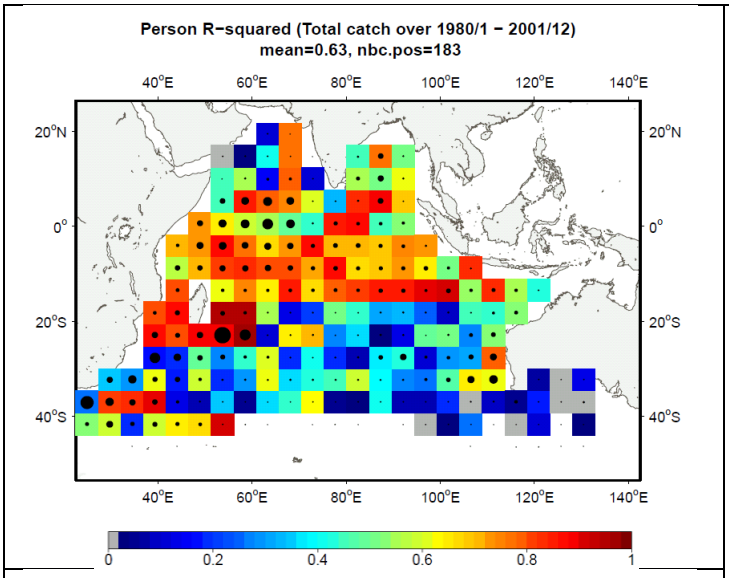

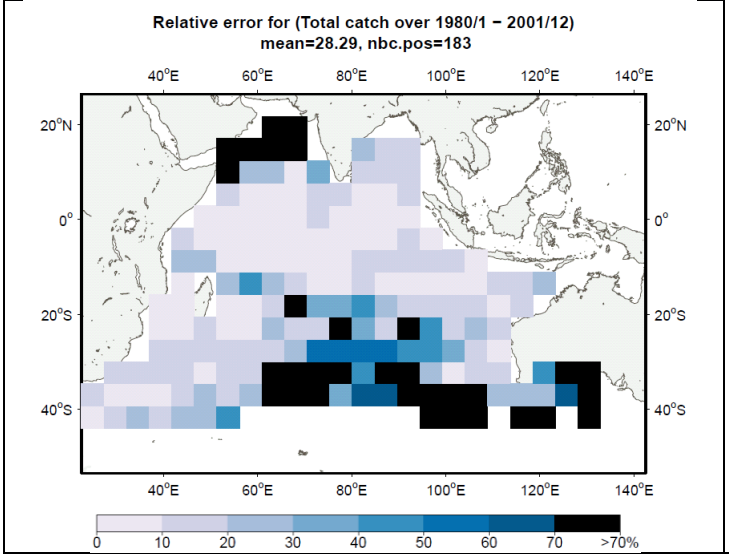

Total predicted and observed catch

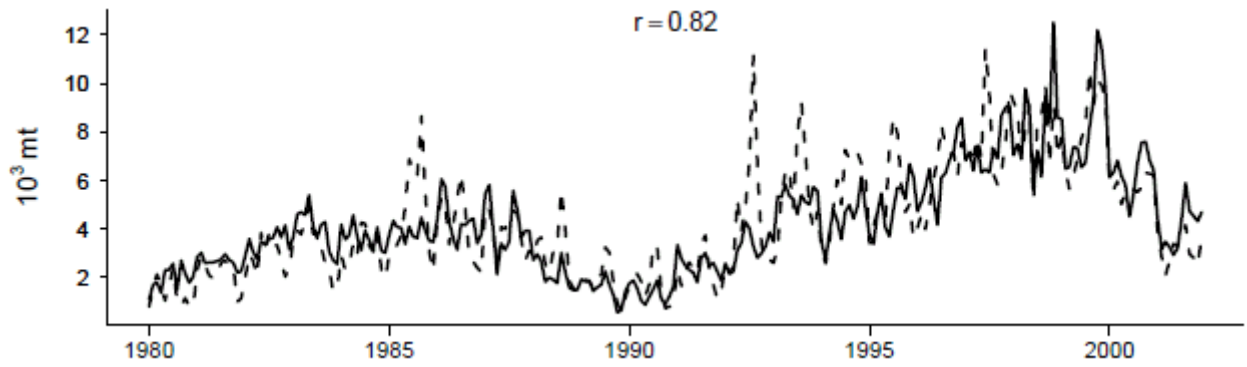

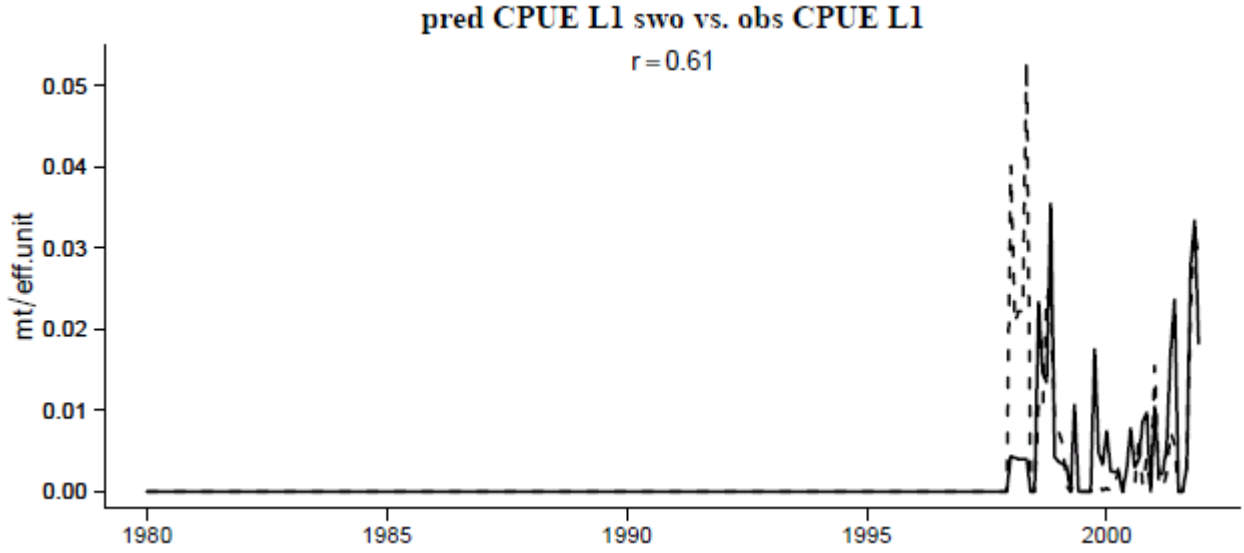
pred CPUE L1 swo vs. obs CPUE L1
r = 0.61
mt/eff.unit
0.05
0.04
0.03
0.02
0.01
0.00
1980
1985
1990
1995
2000

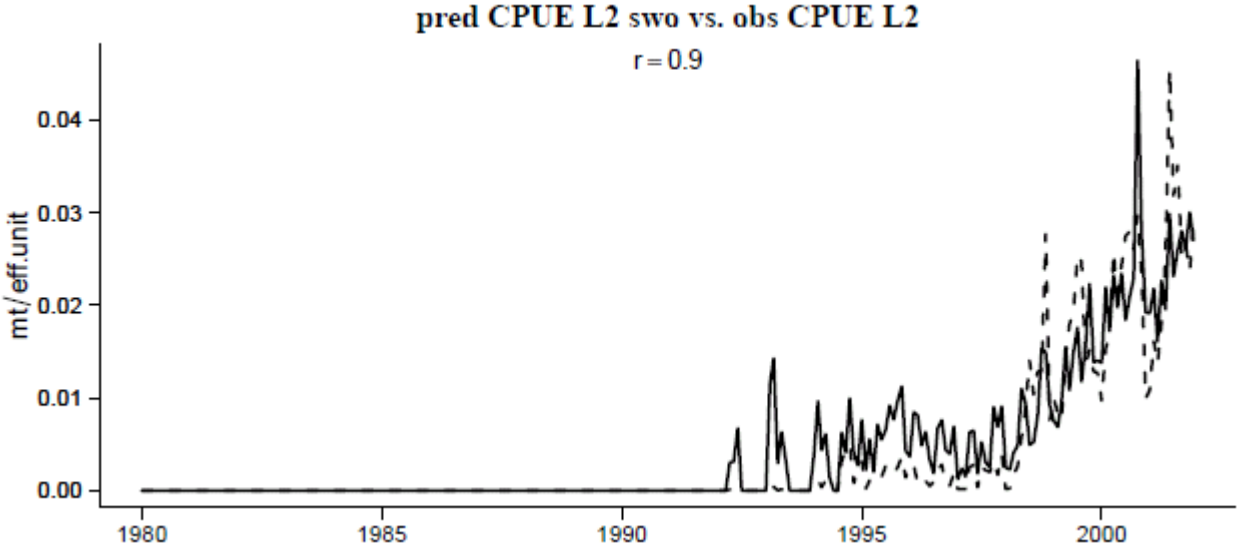
pred CPUE L2 swo vs. obs CPUE L2
r = 0.9
mt/eff.unit
0.04
0.03
0.02
0.01
0.00
1980
1985
1990
1995
2000

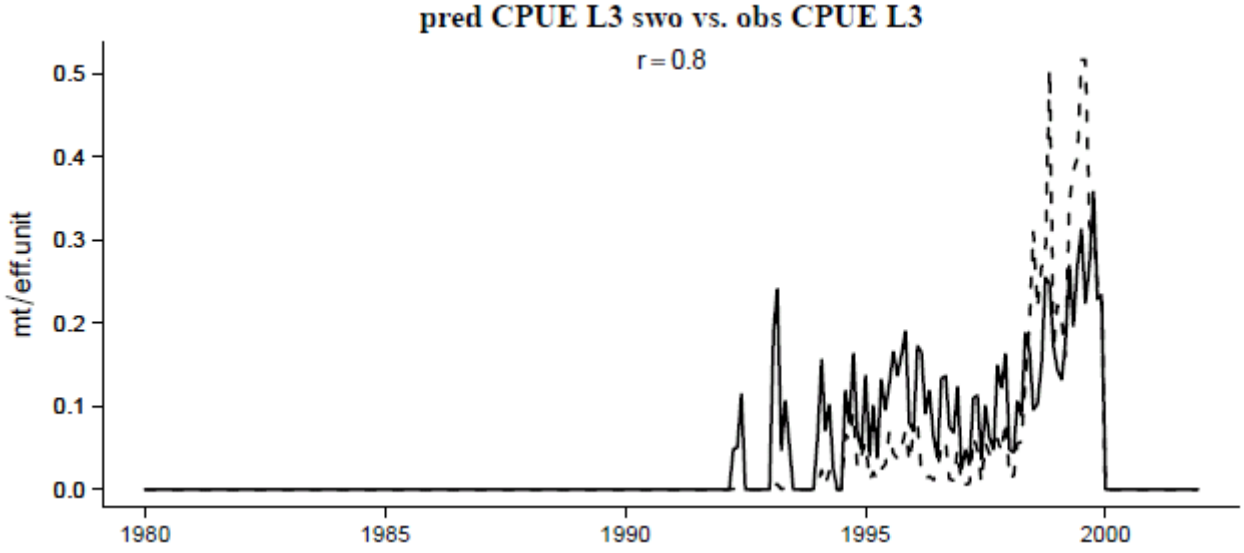
pred CPUE L3 swo vs. obs CPUE L3
r = 0.8
mt/eff.unit
0.5
0.4
0.3
0.2
0.1
0.0
1980
1985
1990
1995
2000

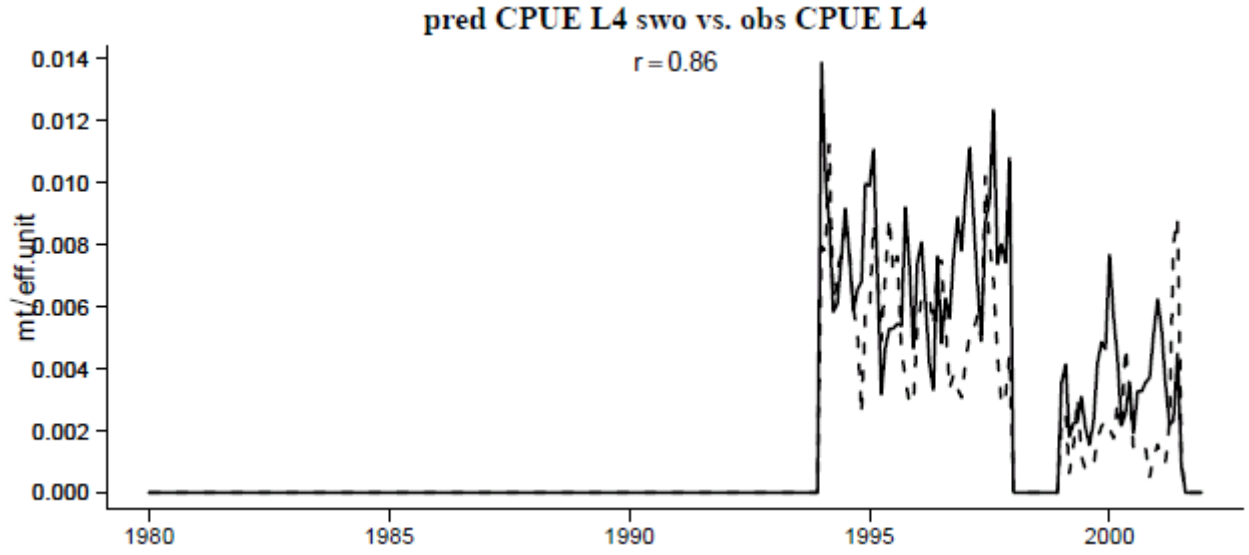
pred CPUE L4 swo vs. obs CPUE L4
r = 0.86
mt/eff.unit
0.014
0.012
0.010
0.008
0.006
0.004
0.002
0.000
1980
1985
1990
1995
2000

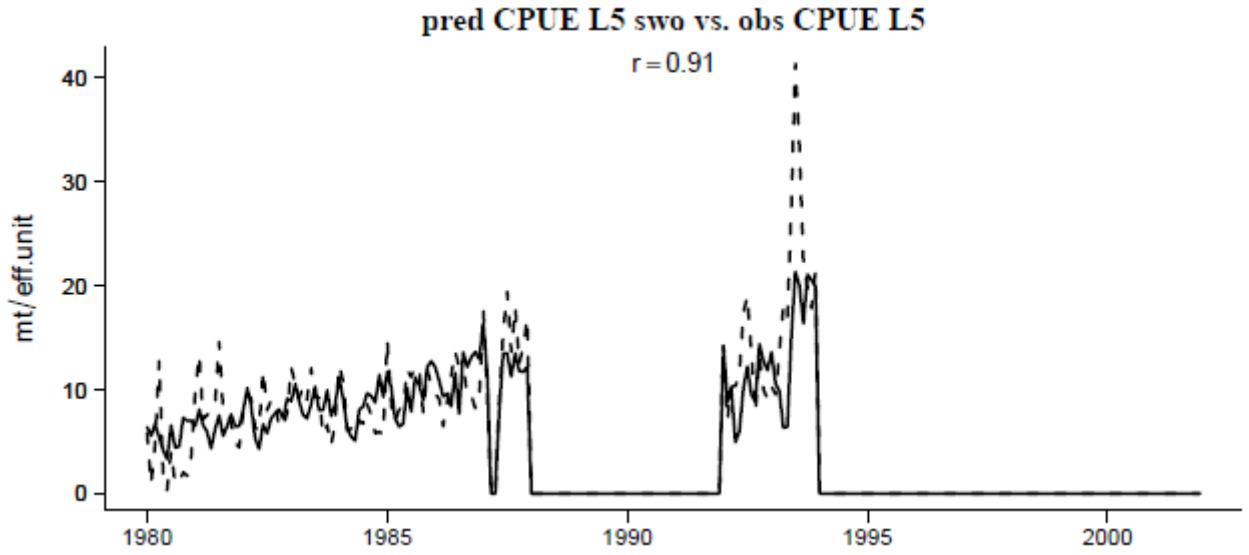
pred CPUE L5 swo vs. obs CPUE L5
r = 0.91
mt/eff.unit
40
30
20
10
0
1980
1985
1990
1995
2000

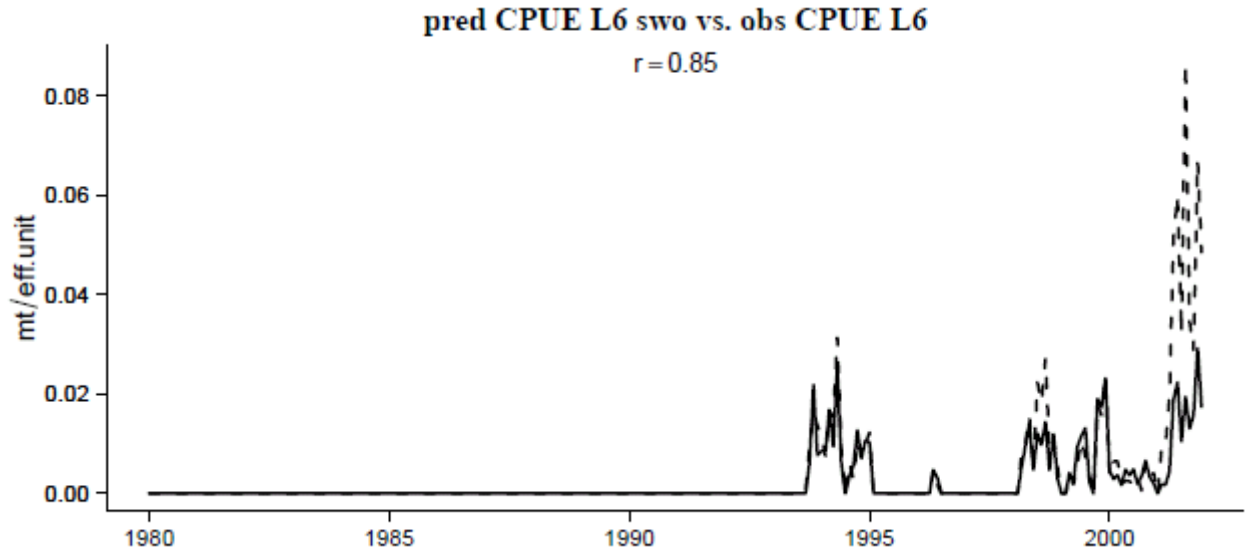
pred CPUE L6 swo vs. obs CPUE L6
r = 0.85
mt/eff.unit
0.08
0.06
0.04
0.02
0.00
1980
1985
1990
1995
2000

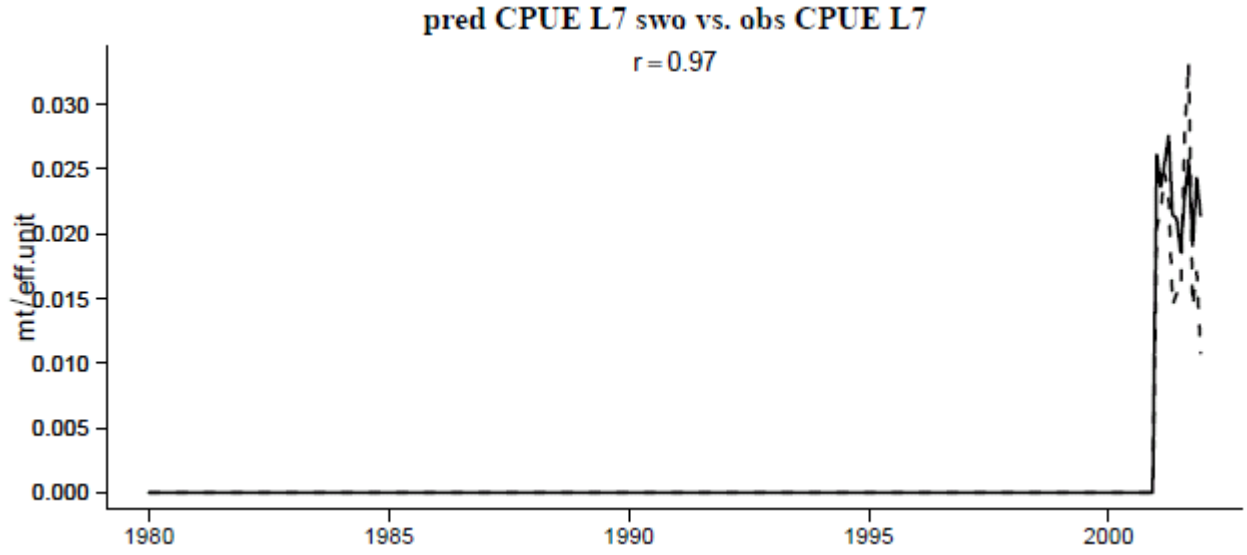
pred CPUE L7 swo vs. obs CPUE L7
r = 0.97
mt/eff.unit
0.030
0.025
0.020
0.015
0.010
0.005
0.000
1980
1985
1990
1995
2000

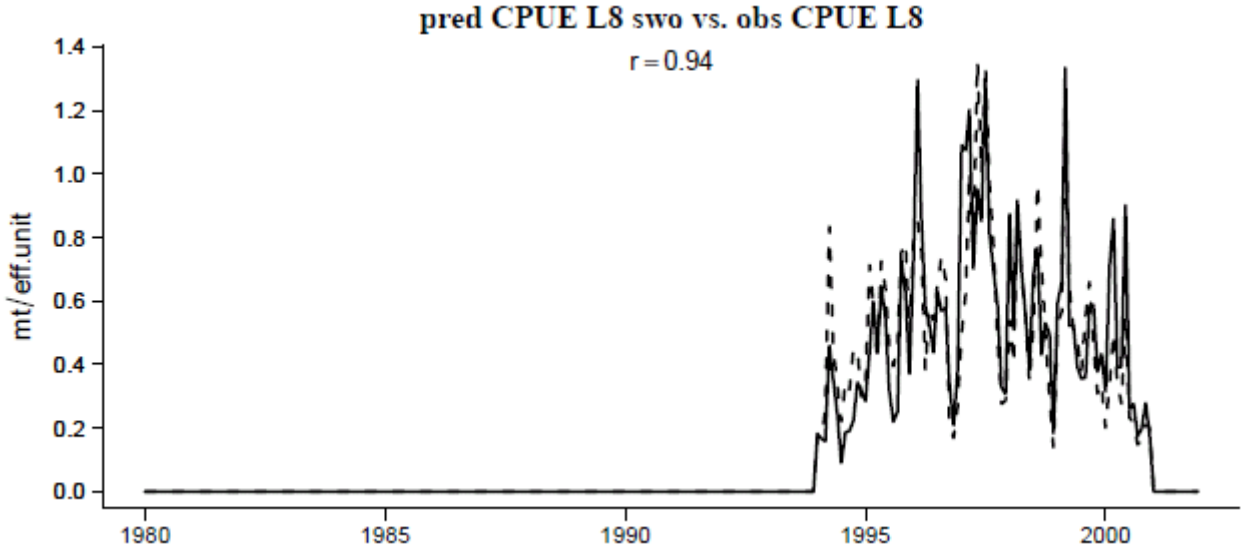
pred CPUE L8 swo vs. obs CPUE L8
r = 0.94
mt/eff.unit
1.4
1.2
1.0
0.8
0.6
0.4
0.2
0.0
1980
1985
1990
1995
2000

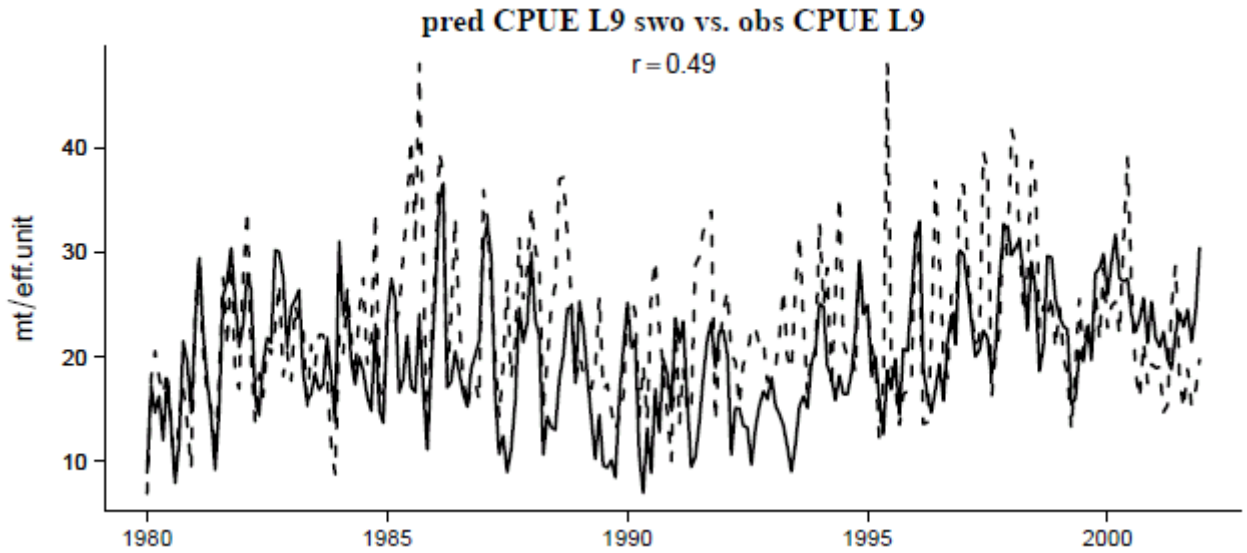
pred CPUE L9 swo vs. obs CPUE L9
r = 0.49
mt/eff.unit
40
30
20
10
1980
1985
1990
1995
2000

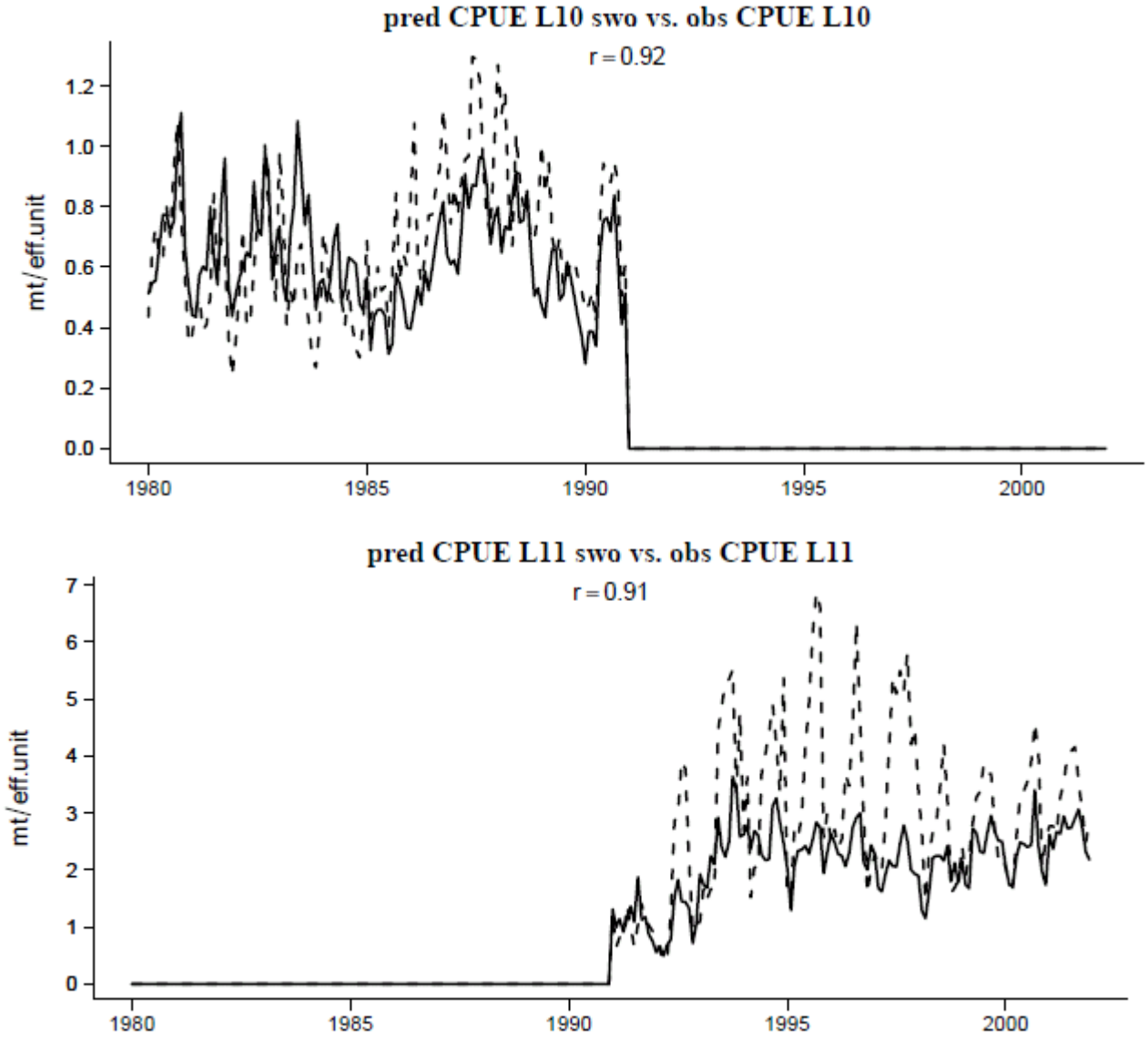

Figure 6. Time series of predicted and observed catch and CPUE by fishery (dashed line: observations, solid line: model predictions) with corresponding size frequency for all the domain and time period (bars: observations, red line: model predictions).

2.5 Parameter estimates

Catchability parameters were the only released parameters. The model converged rapidly and with reasonable estimates of catchability for all fisheries as shown by the fit between observed and predicted CPUEs (Fig. 6). Table 2 presents the Pacific optimal parameterization with which the model converged.

Table 2. Parameter estimates for swordfish application

Parameters estimated by the model			**Unit**	**NCEP-ORCA2**
T_s	Spawning	Optimum of the spawning temperature function	ºC	27.66
α		Larvae food-predator trade-off coefficient		0.43
R		Maximal number of survived larvae per adult	Nb.ind	1.0

b		Beverton-Holt function slope		0.43
T_a	Feeding habitat	Optimum of the adult temperature function at maximum age	^oC	9.5
σ_a		Std. Err. of the adult temperature function at maximum age	^oC	0.9
$\hat{O}$		Oxygen threshold value at Ψ_O =0.5	$mL \cdot L^{-1}$	3.9
M_p	Natural mortality	Slope coefficient in predation mortality		0.06
M_{max}		Senescence mortality at age 0	$month^{-1}$	0.0001
M_s		Slope coefficient in senescence mortality		1.155
D_{max}	Movement	Maximum sustainable speed	B.L. s^{-1}	1.31
s_1		Mid-point of spawning season	day of year	82
s_2		Critical day to night length ratio triggering switch		1.48

*Fixed; [val = value close to minimum boundary value; val] = value close to maximum boundary value

Natural mortality

Natural mortality rates and recruitment are the most difficult parameters to estimate in population dynamics models. For swordfish, recent stock assessment studies used a rate between 0.4/yr (0.033/month) for younger fish and 0.35/yr for fish older than 7 years (Courtney & Piner 2009). For the Pacific Ocean application of SEAPODYM, the estimated natural mortality curve is shown in appendix. The lowest mortality rate (0.012 $month^{-1}$ or 0.15 yr^{-1}) is reached after an age of 3 years and then predicted to slightly increase until 0.05 $month^{-1}$ (0.6 yr^{-1}) for the oldest cohort.

It should be noted that the model allows the average natural mortality coefficients by age to vary locally according to the quality of habitats. As a result, the resulting mortality can vary from the theoretical mean values. The mortality is computed from model outputs using a weighting by cohort density to illustrate the change (cf Fig 7 and Appendix Figure 6 and). For the Indian Ocean application of SEAPODYM, the estimated natural mortality curve is very similar: the lowest mortality rate (0.013 $month^{-1}$ or 0.156 yr^{-1}) is reached after an age of 3 years and then predicted to increase until 0.04 $month^{-1}$ (0.48 yr^{-1}) for the oldest cohort.

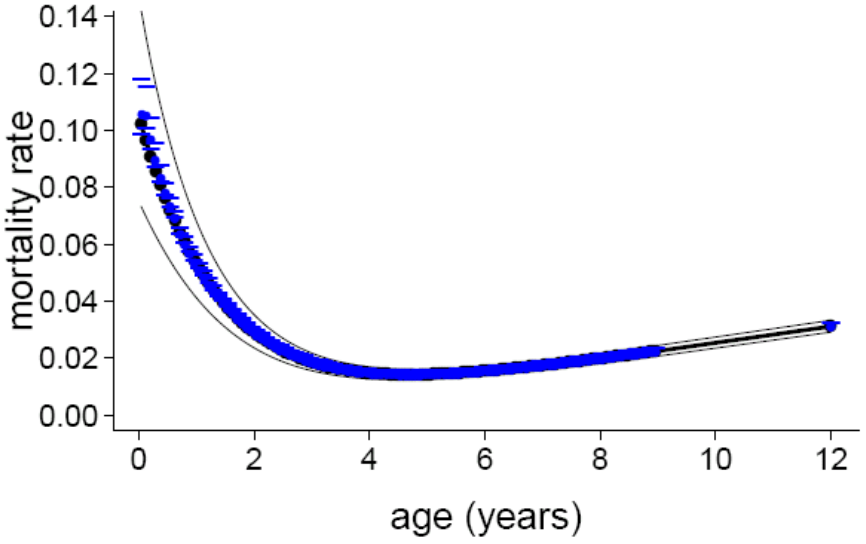

Figure 7. Estimates of average natural mortality rates ($month^{-1}$) by age for swordfish in the Indian Ocean

Habitats, movements and recruitment

As in the Pacific, the model outputs for swordfish in the Indian Ocean suggest opportunistic spawning when SST is higher than 24ºC rather than a well defined spawning period and migration (see details in Appendix Fig. 7, 8 & 9). As a result, the juveniles are mainly predicted to distribute in the Arabian Sea, off the coasts of Somalia, Kenya and Tanzania, with an extension towards the Seychelles Islands (Figure 8).

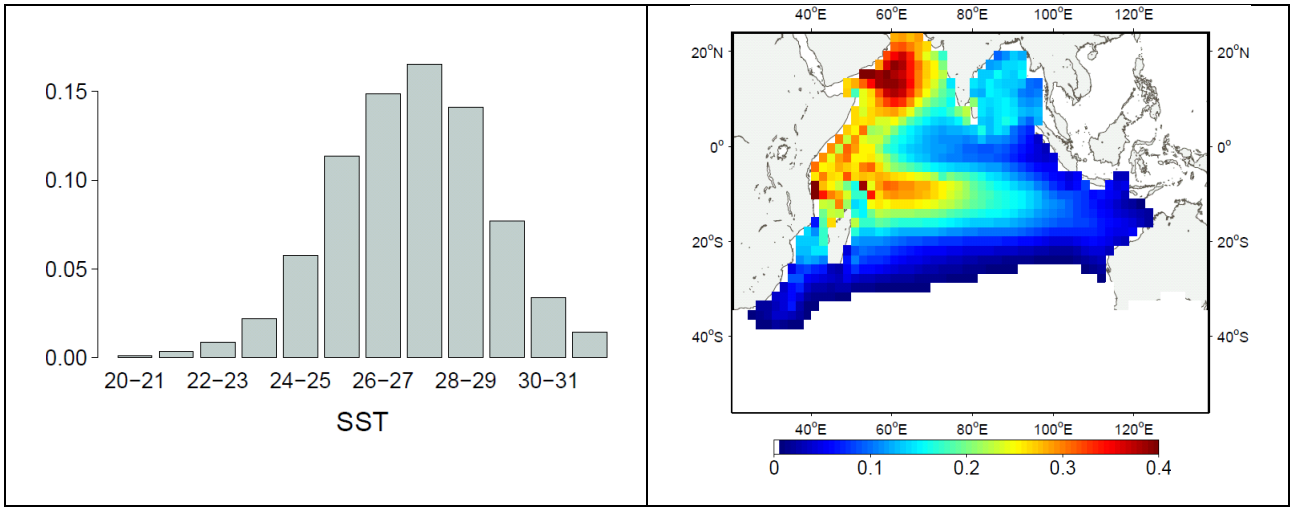

Figure 8. Number of swordfish juveniles as a function of SST (left) and mean monthly distribution of juvenile swordfish (right) for the period 1980-2003).

2.6 Biomass estimates and population dynamics

Predicted distributions of swordfish biomass suggest a large concentration of young immature fish in the Arabian basin, while adult fish is mainly in the southern subtropical region between 20°S and 40°S (Fig. 9). When considering distributions in number of fish rather than in weight (Fig. 10), the contrast is less marked. The catch is distributed in the whole Indian Ocean basin and shows a fairly good overall spatial correlation with the total catch and Japanese CPUE. The seasonal average distributions (Fig. 11) show a seasonal peak in density of juvenile swordfish associated to the third quarter (spring) in the Arabian Sea. This region is also where the highest concentration of young immature fish is predicted all the year (Fig. 11) Adult swordfish are predicted to distribute in the southern subtropical convergence zone, with a seasonal latitudinal movement toward the equator in winter and fall.

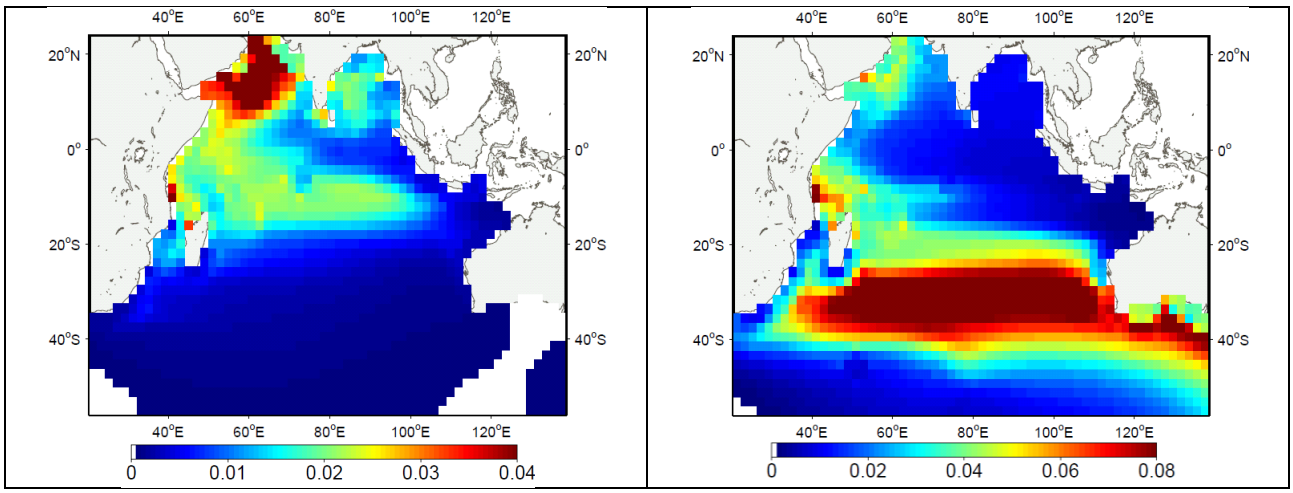

Figure 9: Mean distribution of young (left) and adult (right) swordfish (mt/sq.km) from January 1980 to December 2003.

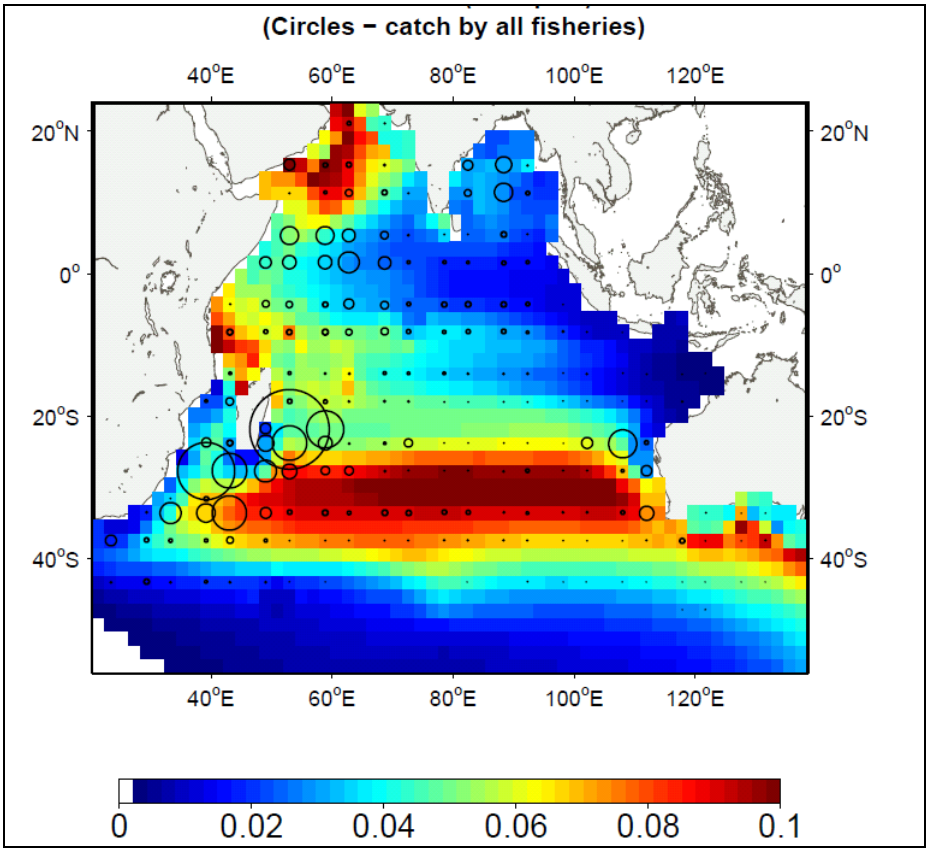

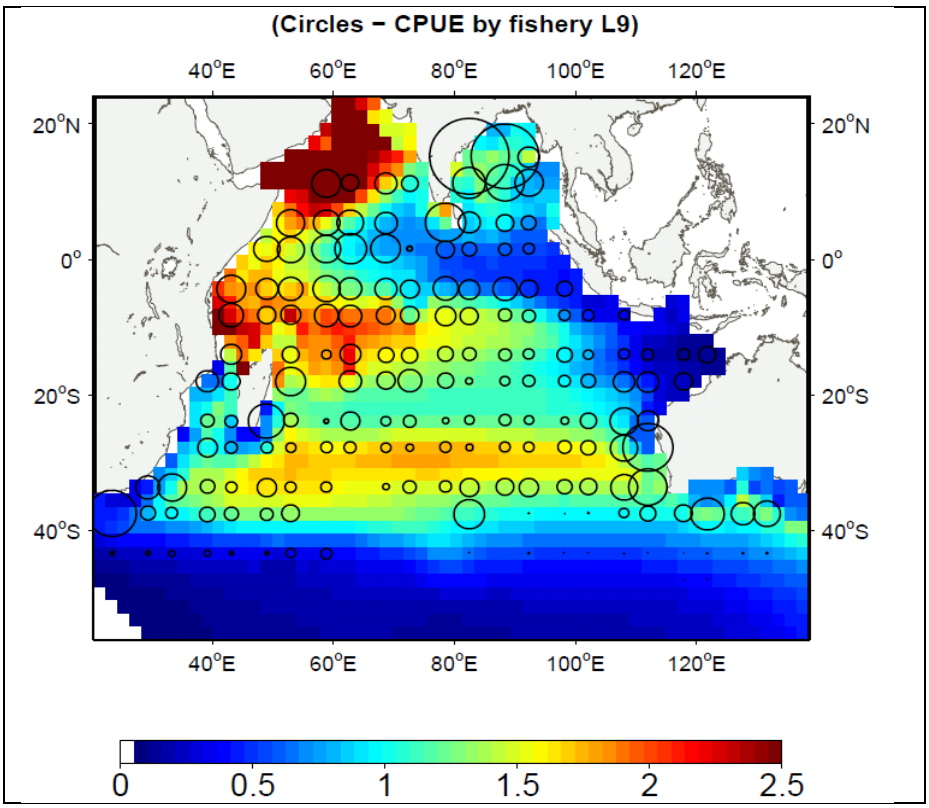

Figure 10. Mean distribution of swordfish (sum of young immature and adult mature fish) with observed catch by fisheries. Top: swordfish biomass in mt km^{-2} and circles proportional to total catch in metric tones. Bottom: Swordfish density in Nb. ind. km^{-2} with circles proportional to average CPUE of Japanese fleet (Nb.ind/100.hooks).

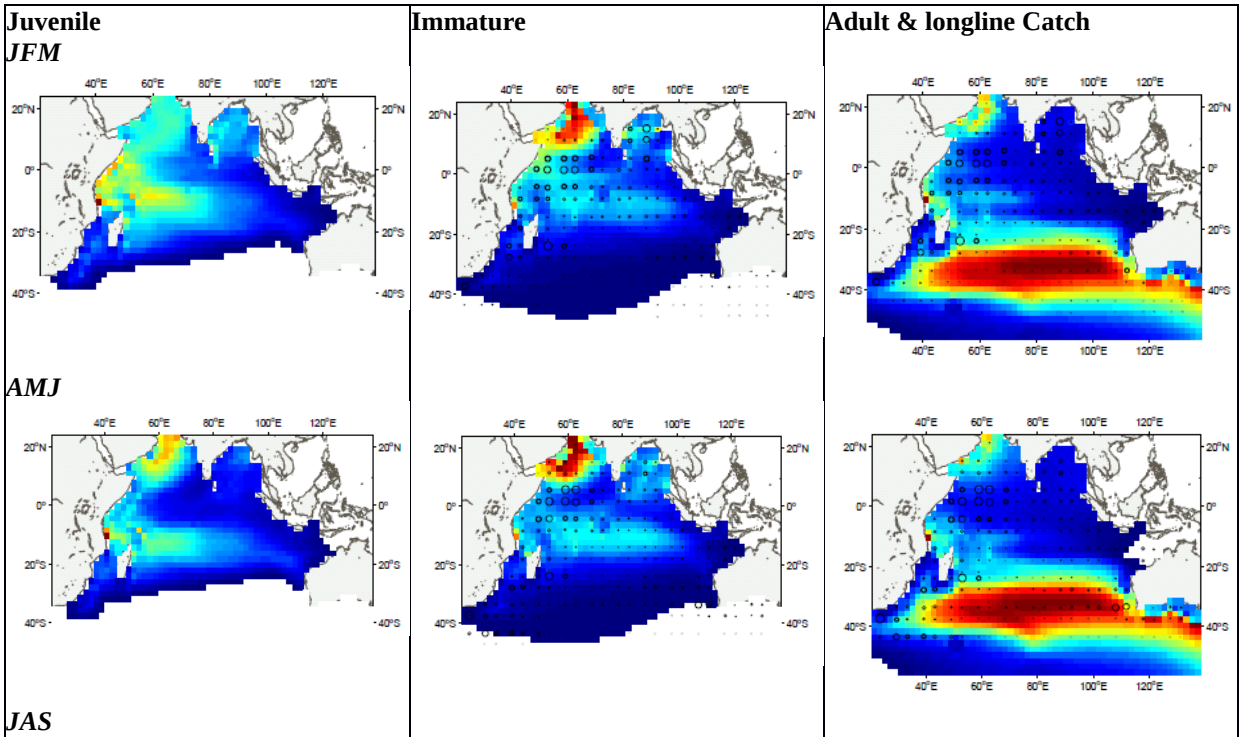

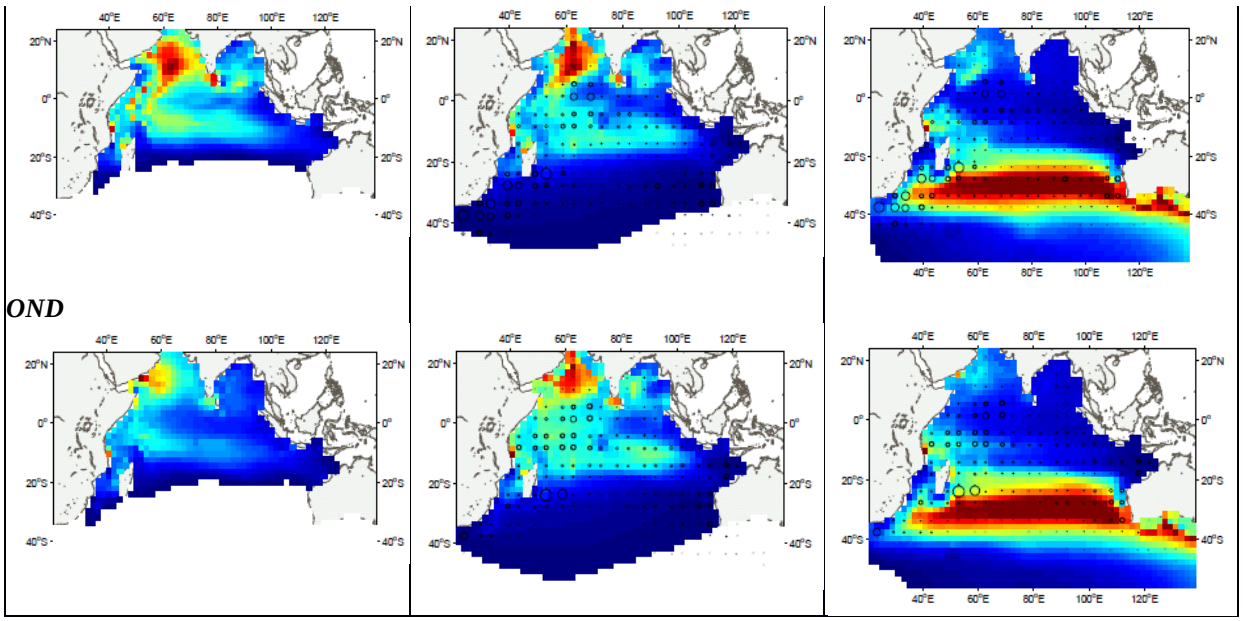

Figure 11. Mean seasonal distribution of young and adult swordfish (Nb / km^2) over the period 1948-2003 with catch superimposed and proportional to the size of circles. JFM stands for January-February-March, AMJ for April-May-June etc.

The overall Indian young and adult stock biomass was estimated between 2.9 and 3.2 millions mt during 1978-2003 period (Figure 12). As for the Pacific stock, this may be overestimated since i) part of the fishing mortality is not taken into account and fisheries selectivity are not properly estimated due to missing length frequency data, ii) the diffusion parameter was estimated to its highest value thus increasing biomass everywhere in the model domain and iii) previous analyses with the model have shown a tendency to increase biomass to achieve a better fit to fishing data, especially when using coarse resolution (e.g. 2°x month) and when fisheries are defined (i.e., aggregated) with too much heterogeneity. Thus, it would be particularly useful to revise this study using higher resolution (eg. 1deg x month) environmental forcing and a complete fishing data set.

On the other hand we can verify given the spatial distributions and population dynamics estimated from the parameter optimization (here from the Pacific application) what can be the minimal stock size allowing the removal of reported catches. Several simulations were run with decreased initial conditions and reproduction rates in order to predict proportionally reduced population abundance with the same trends in the absence of fishing. The results of these simulations are shown in Figures 12 and 13. This methodology allows the estimation of the stock potential range for the entire basin with the minimum biomass needed to explain the catch spatially and temporally. In that case, the total biomass decreases to just below 1 million tones.

Finally, using the same parameterization, a reference simulation without fishing mortality is produced allowing computing the fishing impact (Fig. 13 and 14). As it can be expected the fishing impact is much higher with the minimum biomass estimate and increased from below 10% of total biomass reduction before 1990 to above 30% in the recent years.

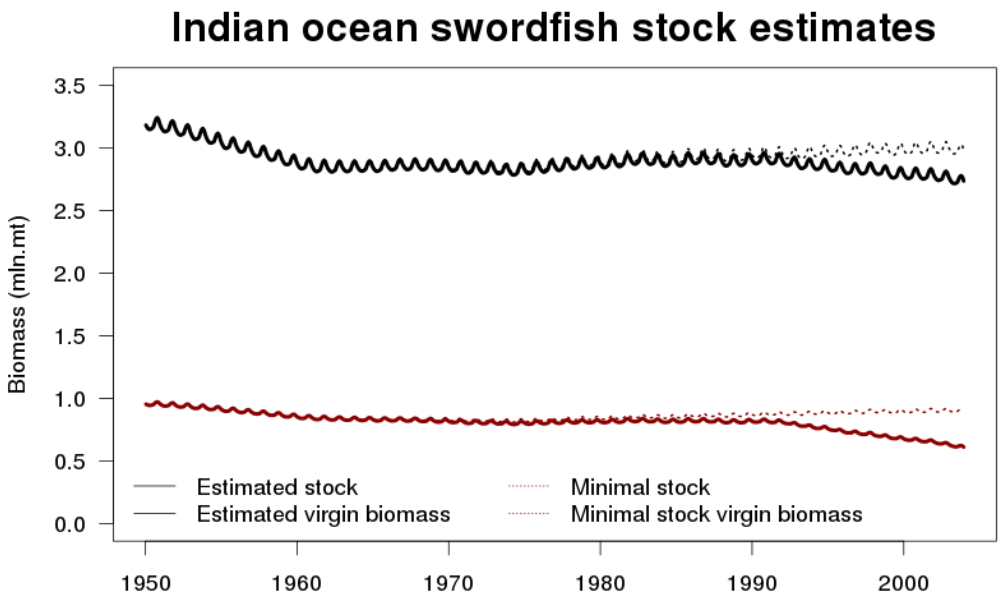

Figure 12. Total Indian swordfish biomass estimate for young and adult cohorts based on the parameter optimization (Pacific application) and after reducing biomass until the minimum level allowing the total catch removal over time and space.

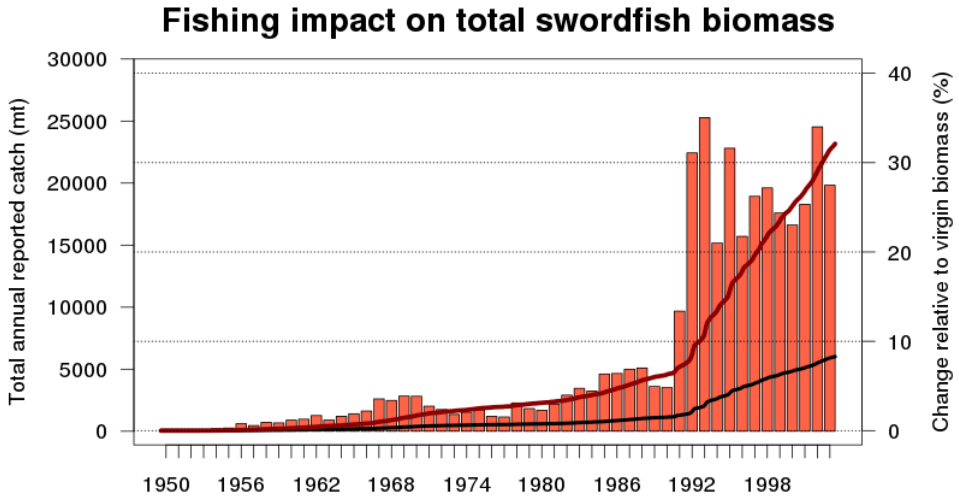

Figure 13. Bars show the total annual catch being used by SEAPODYM. Solid curves show the fishing impact (100*(B(F0)-B)/B(F0)) calculated for two runs (black) estimated population size and (dark red) minimal population size.

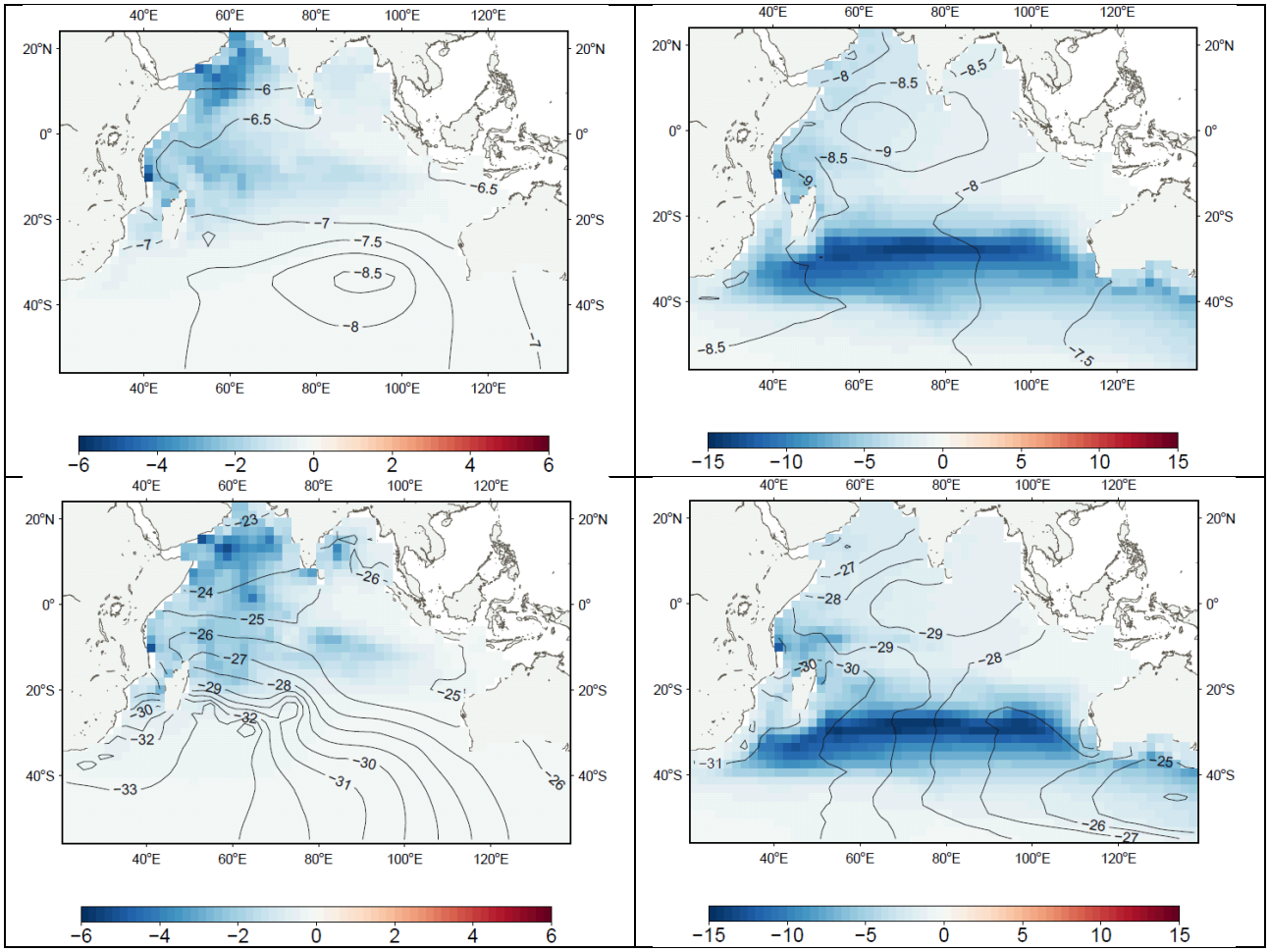

Figure 14. Fishing impact on swordfish given the estimated maximal (top) and minimal (bottom) stock size. The color scale is used to show the average dB = B-B(F0) during the last year of simulation (2003), contour lines showing the percentage of population reduction with respect to virgin biomass B(F0) computed in 2003. Left column - immature cohorts, right column - mature cohorts.

3 Conclusion & Perspectives

This first swordfish application, with minor changes in the optimization of habitats and population dynamics parameters achieved in the Pacific Ocean, was calibrated and validated with catch and effort data of Indian Ocean fisheries. These preliminary results indicate that the proposed solution is already coherent with many features that characterize the swordfish population dynamics and fisheries in the Indian Ocean. The fishing impact was computed using a precautionary approach to estimate the minimum biomass distributed spatially and temporally that allows the removal of observed catch, according to the habitat and population dynamics used in this version.

These preliminary results should be revised and improved with a fully optimized configuration of the model to the Indian Ocean, and using size frequency data in the MLE approach. Given these first encouraging results it should be achievable in a reasonable timeframe. Once the optimal solution will be completed, the model could be used to estimate an average maximum sustainable yield accounting for interannual and decadal variability. Given its spatial structure, it can serve to investigate the connectivity of the stock(s) between any oceanic regions or EEZs. Finally, projections of population trends under different IPCC scenarios of Climate Change could be tested to compute possible change in MSY for the coming decades, and a Indo-Pacific configuration envisaged to increase the fishing dataset and the diversity of environmental conditions used with the MLE framework.

4 References

Abecassis M., Dewar H., Hawn D., Polovina J., 2012. Modeling swordfish daytime vertical habitat in the North Pacific Ocean from pop-up archival tags. Marine Ecology Progress Series, vol. 452: 219-236.

Cerna, J. 2009. Age and growth of the swordfish (Xiphias gladius Linnaeus, 1758) in the southeastern Pacific off Chile. Lat. Am. J. Aquat. Res., 37(1): 59-69, Special issue: "Swordfish fisheries in the southeastern Pacific Ocean

Courtney D, Piner K (2009) Preliminary age structured stock assessment of north pacific swordfish (Xiphias gladius) with stock synthesis under a two stock scenario. Tech. Rep. ISC/09/BILLWG-3/07

DeMartini EE, Uchiyama JH, Humphreys Jr RL, Sampaga JD, Williams HA (2007) Age and growth of swordfish (*Xiphias gladius*) caught by the Hawaii-based pelagic longline fishery. Fishery Bulletin 105:356–367

Dewar H, Prince ED, Musyl MK, Brill RW, Sepulveda C, Luo J, Foley D, Orbesen ES, Domeier ML, Nasby-Lucas N, Snodgrass D, Laurs RM, Hoolihan JP, Block BA, Mcnaughton LM (2011) Movements and behaviors of swordfish in the atlantic and pacific oceans examined using pop-up satellite archival tags. Fish Oceanogr 20:219–241

Hinton M.G., Maunder M.N., 2011. Status of swordfish in the Eastern Pacific Ocean in 2010 and outlook for the future. Inter-American Tropical Tuna Commission, Scientific Advisory Committee, 2nd meeting.

IOTC, 2007, Report of the 10th Session of the Scientific Committee Victoria, Seychelles (5–9 Nov. 2007)

Kolody D, Campbell R, Davies N (2009) South-west pacific swordfish (*Xiphias gladius*) stock assessment 1952-2007. Tech. Rep. WCPFC-SC5-2009/GN-IP-2, WCPFC/CSIRO

Lehodey P, Murtugudde R, Senina I (2010a) Bridging the gap from ocean models to population dynamics of large marine predators: a model of mid-trophic functional groups. Prog Oceanogr 84:69–84

Lehodey P, Senina I, Sibert J, Bopp L, Calmettes B, Hampton J, Murtugudde R (2010b) Preliminary forecasts of population trends for Pacific bigeye tuna under the A2 IPCC scenario. Prog Oceanogr 86:302–315

Lehodey P., I. Senina, B. Calmettes, J. Hampton, S. Nicol, 2013a. Modelling the impact of climate change on Pacific skipjack tuna population and fisheries. Climatic Change, 119:95–109

Lehodey P., I. Senina, O. Titaud, B. Calmettes, S. Nicol, J. Hampton, S.Caillot, P.Williams, 2013b. Report for the Western and Central Pacific Fisheries Commission, Project 62: SEAPODYM applications in WCPO. WCPFC-SC9-2012/EB-WP-03 Rev1. Available at https://www.wcpfc.int/system/files/EB-WP-03-Seapodym-Rev-1.pdf

Poisson F. & C. Fauvel, 2009. Reproductive dynamics of swordfish (Xiphias gladius) in the southwestern Indian Ocean (Reunion Island). Part 1: oocyte development, sexual maturity and

spawning. Aquat. Living Resour. 22, 45–58

Senina I., J. Sibert, P. Lehodey, 2008. Parameter estimation for basin-scale ecosystem-linked population models of large pelagic predators : Application to skipjack tuna. Progress in Oceanography, 78(4), 319:335.

Sibert J., Senina I., Lehodey P., J. Hampton 2012. Shifting from marine reserves to maritime zoning for conservation of Pacific bigeye tuna (Thunnus obesus). Proceedings of the National Academy of Sciences of the United States of America, 109(44), 18221:18225.

Uchiyama JH, Demartini EE, Williams HA (1999) Length-weight interrelationships for swordfish, *Xiphias gladius* L., caught in the central North Pacific. Tech. rep., NOAA/SWFSC

Ward P, Elscot S (2000) Broadbill swordfish: status of world fisheries. Bureau of Rural Sciences, Canberra, Australia

Young J, Drake A (2004) Age and growth of broadbill swordfish (*Xiphias gladius*) from Australian waters. Tech. rep., FRDC & CSIRO

5 Appendix: Optimization based on Pacific swordfish fisheries

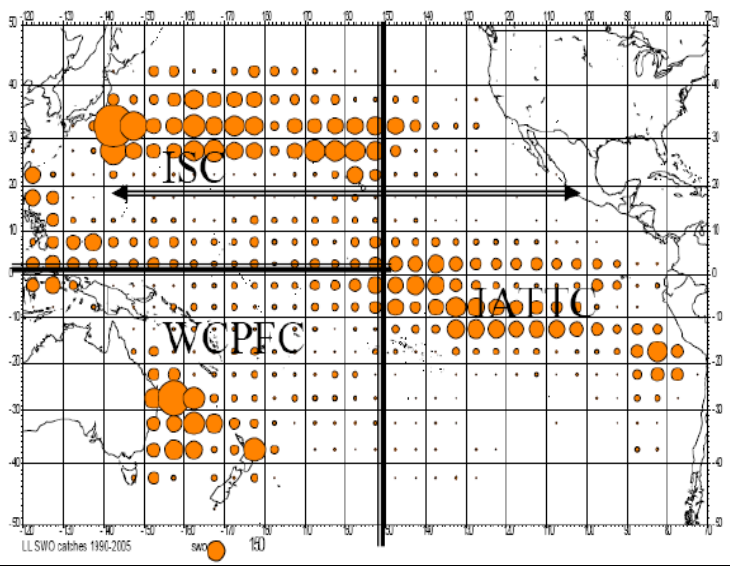

Figure 1

Total swordfish longline catch from 1990-2005 and spatial stratification used for stock assessment by the regional fisheries organizations.

Source: Fonteneau pers.comm.

The swordfish application of SEAPODYM (Spatial Ecosystem And Population Dynamic Model) was optimized in the Pacific Ocean during a collaborative project between CLS, the Secretariat of the Pacific Community (SPC) and the PIFSC/NOAA (Hawaii, USA). The environmental forcing NCEP-ORCA2 was chosen to cover both the historical period of swordfish fisheries and several lifespan of the species. Available catch per unit of effort (CPUE), effort, and length-frequency data from the fisheries operating in the study area were assimilated into the model. However, only a partial coverage of fishing data was accessible.

Several stocks or sub-stocks seem to emerge from the spatial representation of total catch data (Fig. 1): one stock in the eastern Pacific mainly in the equatorial region with a south-eastern extension reaching the coast of Peru and Chili; a south-western stock between Australia and New Zealand and the northern stock in the Kuroshio extension with a possible link to the tropical western Pacific sub-stock. Currently the stock assessment studies conducted by the regional fisheries organization are based on this 3-stock hypothesis (Kolody et al. 2009; Hinton & Maunder 2011; Courtney and Piner 2009).

1. Fishing data

The fishing data sets available for this study were catch data provided by NOAA/NMFS for the Hawaii-based longline fisheries and low-resolution public domain spatially-disaggregated monthly catch data provided by SPC. Quarterly length frequency data associated with each fishery over the historical fishing period were also available. Table 1 summarizes the fishing data included in this analysis. Fishing data provided by NMFS for 3 Hawaii-based longline fisheries were at the resolution of the model (2ºx2ºx month). The SPC catch and effort data were 5ºx5ºx1 month aggregated by flag. Figure 1 shows the composition of catch by flag for the WCPFC member countries. The Japanese, Korean, Taiwanese and Australian fisheries, along with the Hawaiian fisheries represent nearly 100% of the catch in the WCPO. However, at the scale of the whole Pacific Ocean, and especially for the recent period, important fisheries are missing, in particular those of Mexico, Spain, Chile, and Peru (Courtney & Piner 2009; Hinton & Maunder 2011). Australian data prior to 1996 were not used, as

they represent a period during which the swordfish longline fishery was developing in Australia, with a switch to bigger boats and better targeting of swordfish (Ward & Elscot 2000). Such abrupt changes in fishing techniques make the data unsuitable for the optimization as the model defines a unique constant catchability parameter per fishery, with an optional constant linear trend.

Until the end of the 1980s the catch of Pacific swordfish was essentially due to the Japanese longliners (Fig. 2). Then several other longline fisheries progressively increased their fishing effort and catch of swordfish either as a target species or bycatch, while conversely the Japanese longline catch decreased, but still represented roughly half of the total catch in 2000 and about 1/3 in 2008.

Table 1. Fisheries definition for the Pacific swordfish.

ID	Gear	Region	Description	Nationality	available catch/effort	Resolution	available LF	Resolution
L1	LL	171°- 234°E 2°N- 46°N	night-time shallow sets targeting swordfish	US (Hawaii)	1995-2010	1° x 1°	171°- 234°E 2°N- 46°N	1°x1°
L2	LL	174°-238°E 0°N- 46°N	mixed sets targeting swordfish	US (Hawaii)	1995-2006	1° x 1°	174°E-238°E 0°N- 46°N	1°x1°
L3	LL	182°E-232°E 17°N- 42°N	daytime deep sets targeting bigeye tuna	US (Hawaii)	1995-2010	1° x 1°	182°E-232°E 17°N- 42°N	1°x1°
L4	LL	102.5° - 122.5°E 47.5°S - 2.5°N	pooled LL	Japan	1950-2008	5°x5°	102.5° - 122.5°E 47.5°S - 2.5°N	5°x5°
L5	LL	102.5°E - 287.5°E 62.5°S - 62.5°N	pooled LL	Korea	1962-2008	5°x5°	142.5° - 237.5°E 12.5°S - 12.5°N	5°x5°
L6	LL	102.5 – 282.5 E -42.5 – 47.5 N	pooled LL	Taiwan - ROC	1958-2008	5°x5°	102.5° - 222.5°E 17.5°S - 17.5°N	5°x5°
L7	LL	142.5 – 172.5 E 47.5 - 12.5 S	pooled LL	Australia	1996-2008	5°x5°	NA	NA

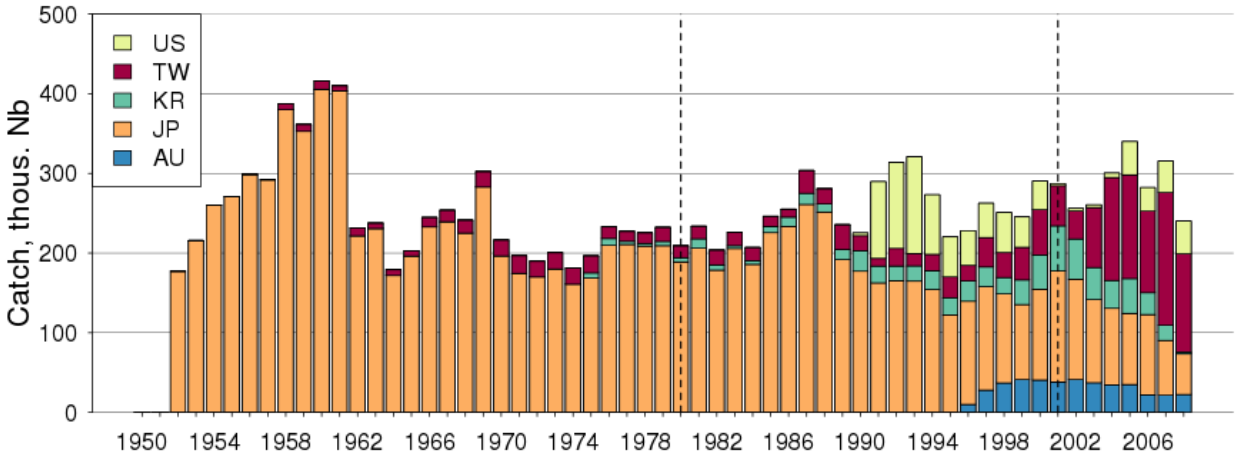

Figure 2. Swordfish annual catch by flag. Data provided by SPC for the whole Pacific Ocean for the main contributors to the swordfish fisheries. Vertical lines show the limits of the dataset used in parameter estimation (1980 – 2001).

2. Optimization experiments

The parameter estimation was conducted using historical (available, spatially distributed) fishing dataset over the period 1980-2003. Model predictions were aggregated on the resolution of the data (5° x month) before contributing to the likelihood. The optimization method converged providing the estimates of 13 population dynamics parameters (see more details in section 5, Table 2) and 23 fisheries parameters. The optimal solution has a reasonable fit to catch data (see more details in section 4, Fig 4).

3. Population structure

The model simulates age-structured swordfish populations with one length and one weight coefficient per age cohort (males and females combined) obtained from independent studies. The SPC LF data was converted from lower-jaw fork length (LJFL) to eye fork length (EFL) to be consistent with the growth curve and the Hawaii LF data. We used the average between three different growth curves from the central Pacific (DeMartini et al 2007), Australia (Young & Drake 2004) and the eastern Pacific (Cerna 2009). The weight curve was derived from the length-weight relationship in Uchiyama et al. (1999).

Sexual dimorphism occurs for swordfish with large differences between the growth rate, the size and the age at maturity of males and females (DeMartini et al 2007, Ward & Elscot 2000). Females live longer, grow faster after the third year and reach larger sizes. They also mature later. The different sexes may also have different spatial distributions (Ward & Elscot 2000). The present SEAPODYM version doesn't allow two different sets of parameters for males and females, so the biological parameters had to be averaged between males and females.

Due to the very rapid growth of swordfish during the first months of life and the monthly resolution of our forcing, the age structure was defined as follows: no larvae class; one monthly age class for juveniles; and 13 adult cohorts of varying durations - 8 for immature adults up to age 3 yr, when 50% of the fish are sexually mature (we used the mean age at maturity for females as they are considered to represent the spawning biomass, Ward & Elscot 2000), and 5 cohorts for mature adults up to age 9 yr with older fish accumulating in the last cohort (Fig. 3). After the juvenile phase, swordfish become autonomous, i.e., they have their own movement (linked to their size and feeding habitat) in addition to being transported by oceanic currents.

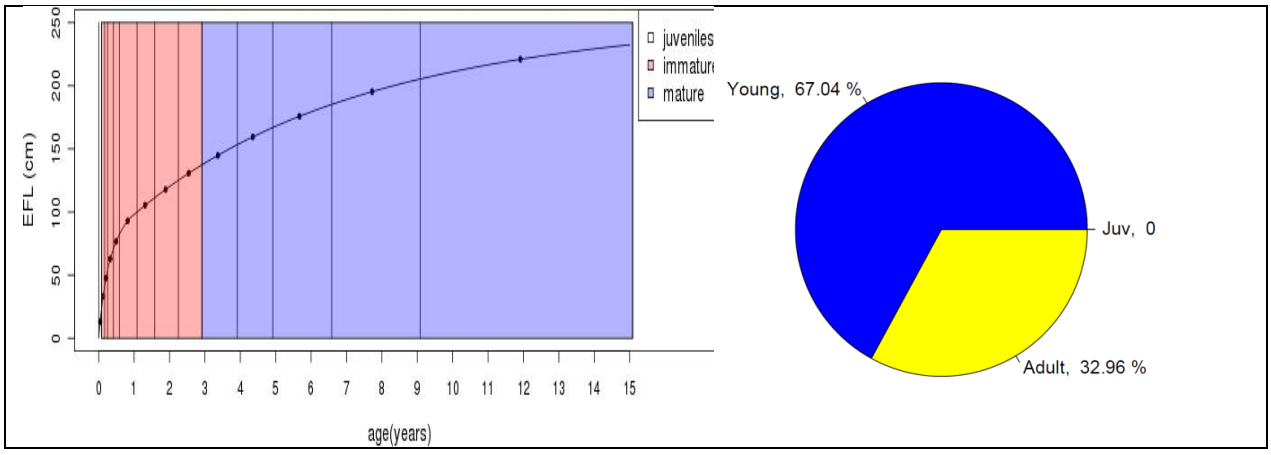

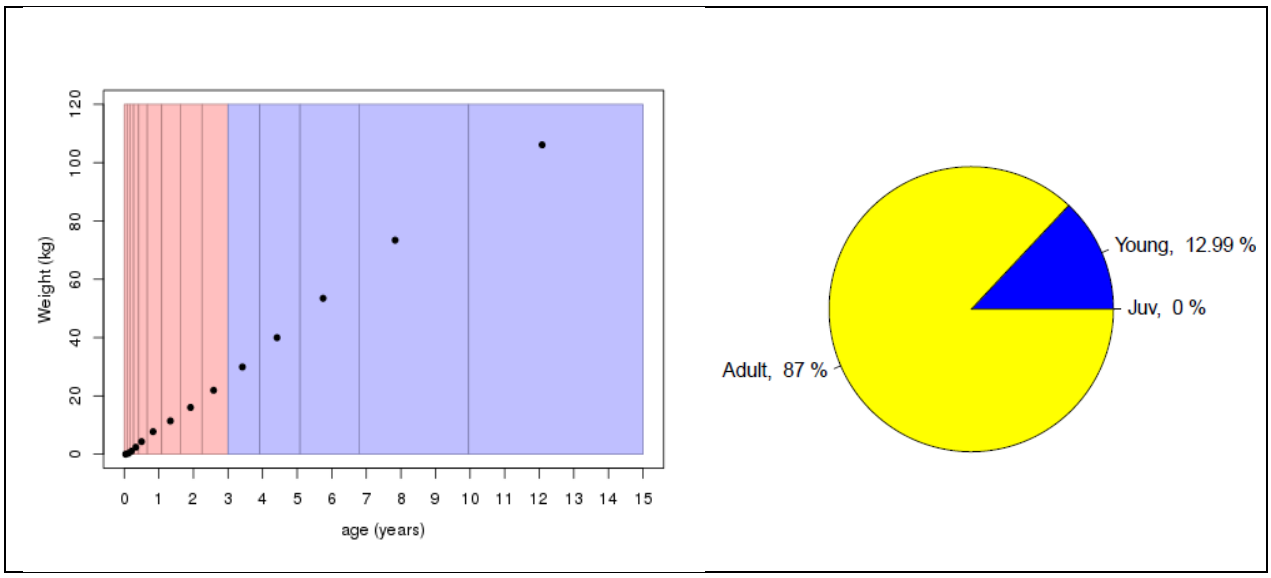

Figure 3. Age structure used in the swordfish configuration. Average length (top-left) and weight (bottom-left) as being found in the literature and estimated stage composition in number of fish (top) and biomass (bottom) by life stage.

4. Fit to catch data

The overall spatial coverage of effort and catch data encompasses all the Pacific Ocean between 45°N and 45°S (Fig. 4). Except for a few exceptions, the poorly fitted areas correspond to areas of low levels of catch, outside of the main swordfish fishing grounds described above from Fig 1. The variance is relatively well explained by the model and relative error on predicted catch significant only in cells of very weak catch and effort (Fig 4). Around Hawaii islands, the fit is particularly high with the fishing data that were provided at the resolution of the model grid, highlighting the importance of a good accuracy in fishing data. Beside, the Hawaiian longline fisheries (L1, L2 and L3) get high correlation over time for catch and CPUE and a good match also between observed and predicted size frequencies of catch (Fig. 5). The fishery L3 targeting bigeye tuna is much less selective in the size of swordfish bycatch. The fit between predicted and observed catch and CPUE still remain good for other fisheries but a good match for size frequencies of catch is difficult to achieve, likely due to a lack of homogeneity in the data mixed in one single longline fishery. As for Hawaiian fisheries it would be necessary to access to a better definition of fisheries by target species and fishing strategy (e.g., deep or shallow sets). For Australian fishery (L7), data prior to 1996 were excluded. After this year, the fishery can be considered mature and homogeneous. The fit achieved for this fishery is high but unfortunately no size data were available.

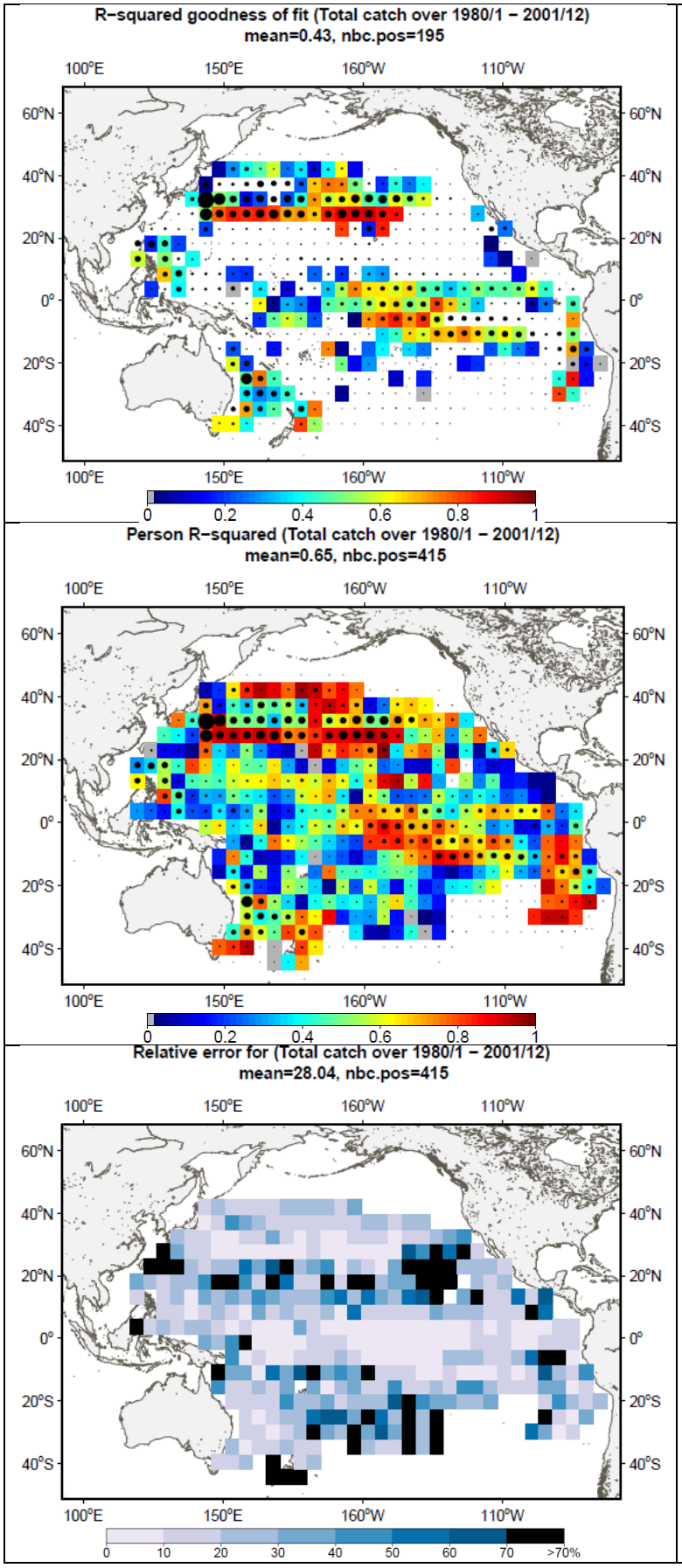

Figure 4. Spatial fit to catch data.

Top: Map of R-squared goodness of fit metrics representing the spatial fit over the period used for optimization (white squares indicate negative correlation between observations and predictions), overlaid with the total catch in each cell (black circles proportional to catch)

.

Middle: Map of Pearson r-squared metric, which quantifies the percentage of the catch variance explained by the model in each cell, overlaid with the number of observations (fishing events).

Bottom: Map of the mean error.

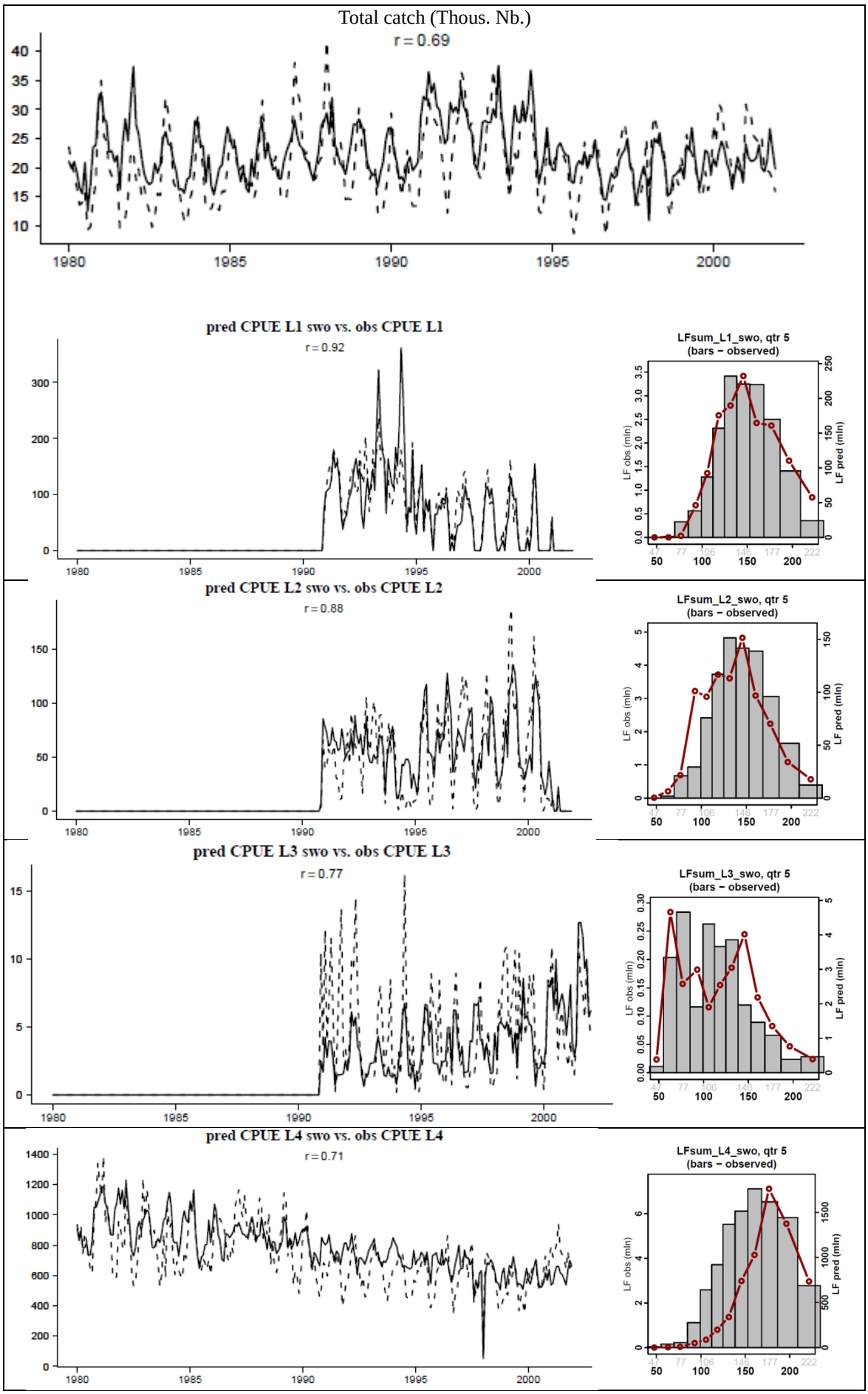
Total catch (Thous. Nb.)
r = 0.69
pred CPUE L1 swo vs. obs CPUE L1
r = 0.92
LFsum_L1_swo, qtr 5
(bars – observed)
LF obs (mln)
LF pred (mln)
pred CPUE L2 swo vs. obs CPUE L2
r = 0.88
LFsum_L2_swo, qtr 5
(bars – observed)
LF obs (mln)
LF pred (mln)
pred CPUE L3 swo vs. obs CPUE L3
r = 0.77
LFsum_L3_swo, qtr 5
(bars – observed)
LF obs (mln)
LF pred (mln)
pred CPUE L4 swo vs. obs CPUE L4
r = 0.71
LFsum_L4_swo, qtr 5
(bars – observed)
LF obs (mln)
LF pred (mln)

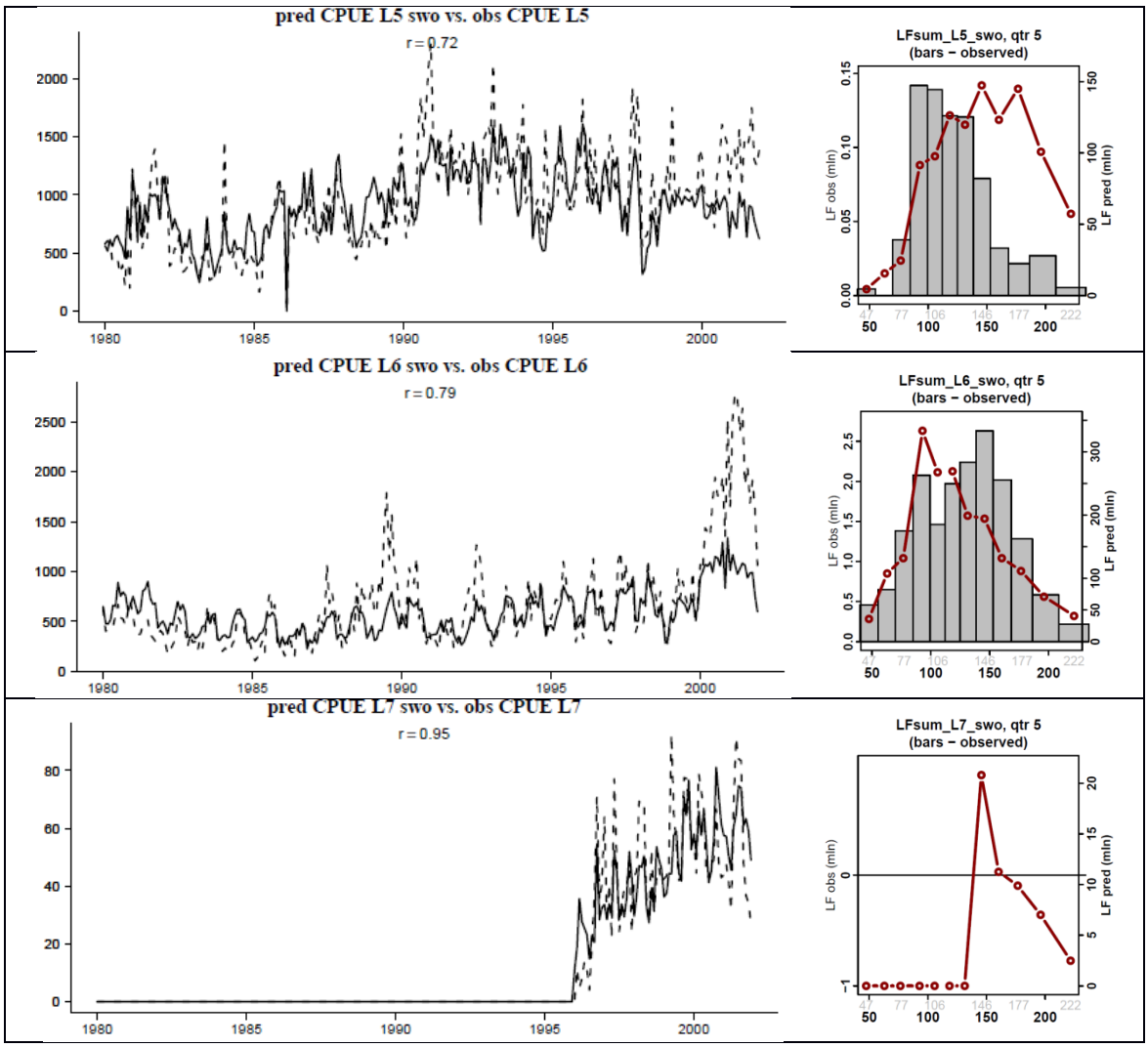

Figure 5. Time series of predicted and observed catch and CPUE by fishery (dashed line: observations, solid line: model predictions) with corresponding size frequency for all the domain and time period (bars: observations, red line: model predictions).

5. Optimal Parameterization

The model converged with reasonable estimates for most parameters, but a few of them had still to be fixed or reached the boundary values.

Natural mortality

Natural mortality rates and recruitment are the most difficult parameters to estimate in population dynamics models. For swordfish, recent stock assessment studies used a rate between 0.4/yr (0.033/month) for younger fish and 0.35/yr for fish older than 7 years (Courtney & Piner 2009). The estimated natural mortality curve with SEAPODYM is shown in Fig. 6. The lowest mortality rate (0.012 month^{-1} or 0.15 yr^{-1}) is reached after an age of 3 years and then predicted to slightly increase until 0.05 month^{-1} (0.6 yr^{-1}) for the oldest cohort.

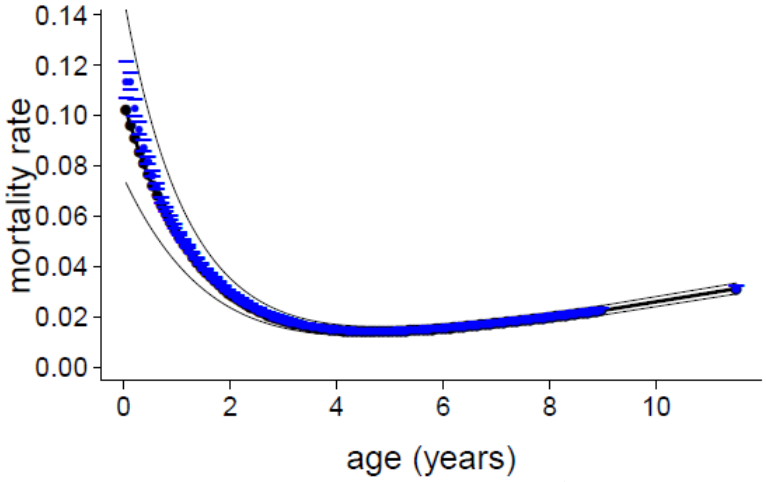

Figure 6. Estimates of average natural mortality rates (month^{-1}) by age for swordfish in the Pacific Ocean

Spawning and juvenile recruitment

The estimated optimal temperature (27.66ºC) for spawning (Fig 7) is in agreement with published values since swordfish are known to spawn in waters with sea surface temperature between 24 and 29 ºC (Ward & Elscot 2000). The standard error of the spawning temperature function had to be fixed (1.5°C). Swordfish do not seem to have a specific spawning period but rather spawn whenever SST is higher than 24ºC. At higher latitudes, this limits spawning to spring and summer. The model estimate for the seasonal timing of spawning migration indicates that the switch from feeding to spawning habitat controlling the movement of fish peaks at Julian date 81.75 (21 March) in the north hemisphere, i.e. exactly at the spring equinox (Fig 7c). The switch occurs earlier in higher latitudes. Movement of fish between latitude 34.5°N - 34.5°S is always controlled by the feeding habitat while spawning occurs year-round opportunistically and proportionally to the spawning habitat index and the density of adult fish (Fig 7d), following the larval stock-recruitment relationship expressed in SEAPODYM, ie at the cell level.

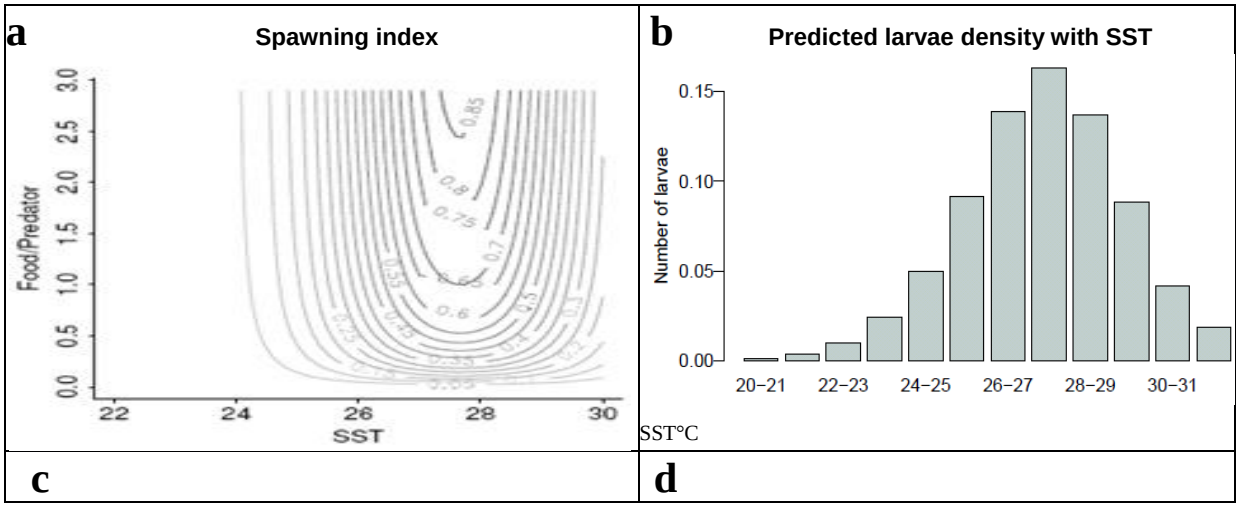

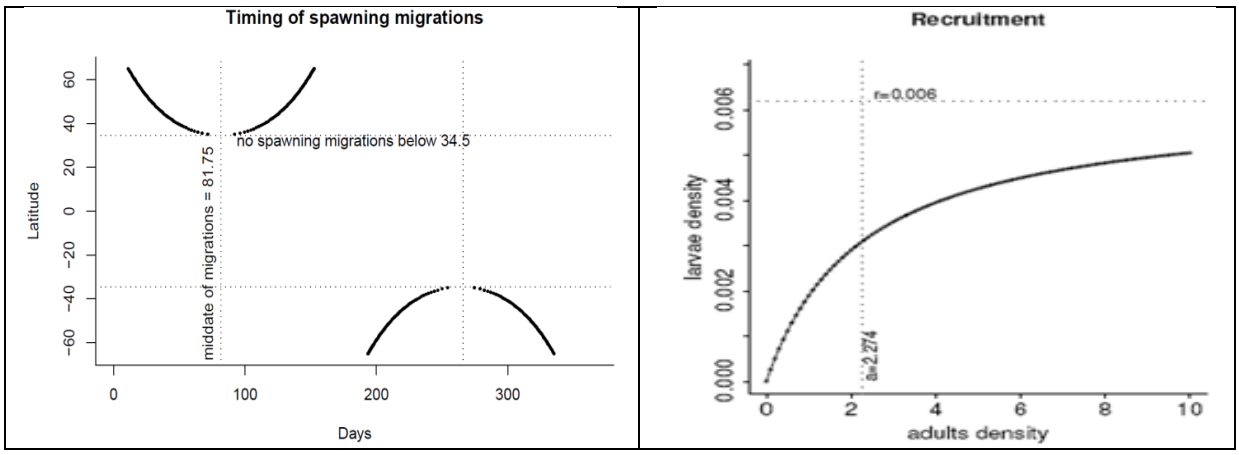

Figure 7: Spawning and larval recruitment. **a:** spawning index in relation to SST and food-predator tradeoff ratio. **b:** Distribution of larvae according to SST and the estimated parameters of spawning index.c: Seasonal timing of spawning migration. **d:** SEAPODYM larval stock-recruitment relationship estimated for swordfish. Densities are in number of individual per km^2 for adult and 1000's of individual per km^2 for larvae.

Feeding habitat

The thermal habitat by age resulting from the optimization experiment is shown on Fig. 12.8. Based on previous optimization experiments for tuna, the optimal feeding habitat temperature of the oldest cohort is usually difficult to estimate. However here, a reasonable value was obtained (9.5°C). The estimated threshold in dissolved oxygen (~3.9 mL/L) seems quite high since satellite tracking data suggest that swordfish are more tolerant to low ambient dissolved oxygen concentration than most tuna species (Abecassis et al 2012, Dewar et al. 2011). This high oxygen threshold value may reflect the partial representation of catch (i.e., presence) in the eastern Pacific, since this region is marked by the most shallow oxygen minimum layer.

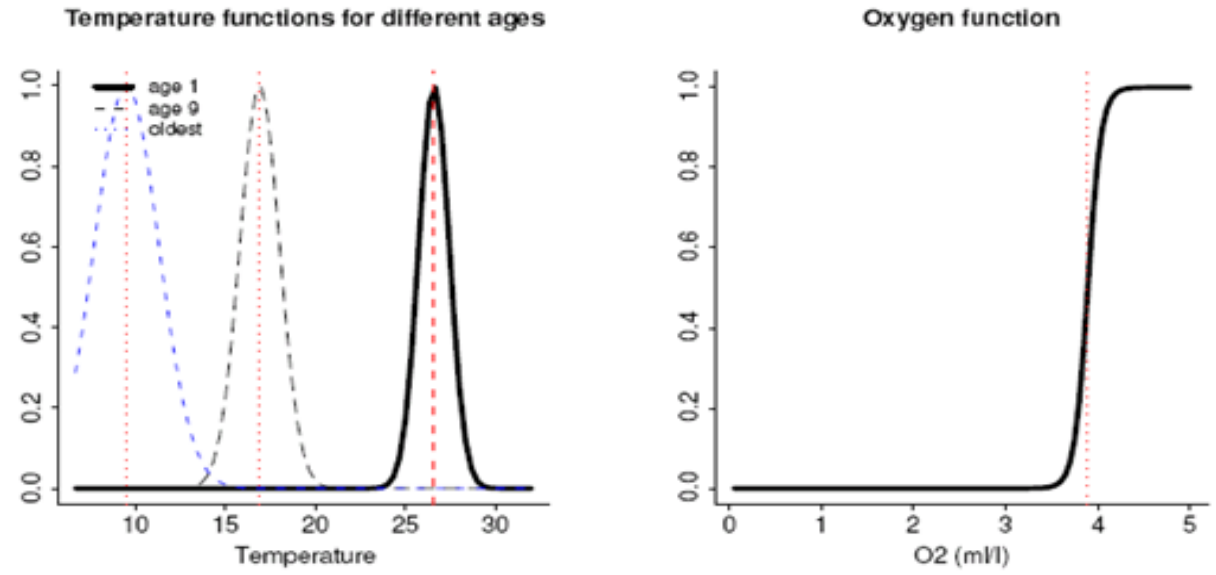

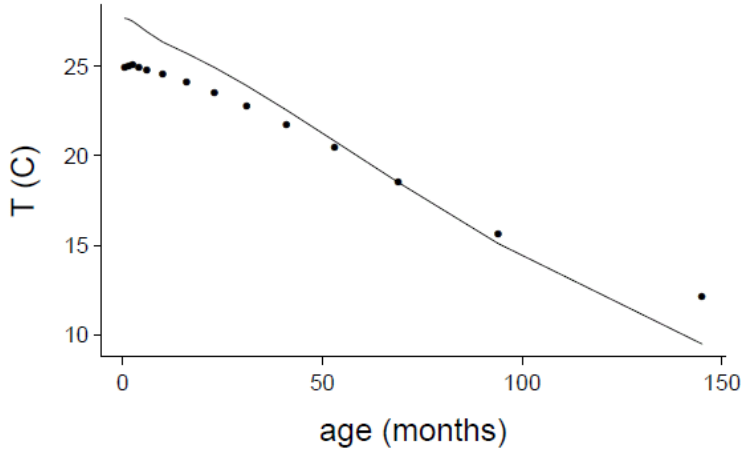

Figure 8: Estimated temperature and oxygen indices (top) and mean ambient temperature computed as a weighted average of swordfish biomass (bottom)

Movements

The model was able to estimate the maximum sustainable speed parameter at a theoretical value of 1.3 BLs^{-1} but the diffusion coefficient for fish movements reached the upper boundary. As for other optimization experiments with tuna, this latter parameter is difficult to estimate, because in absence of key information the model has a tendency to increase diffusion to facilitate the fit with catch data due to the strong correlation of catch with fishing effort. When weighted by the cohort density, maximum diffusion rates are still rather high but remain below 4000 nmi^2 day^{-1} and the mean of maximum sustainable speed (in BL/s) is between 0.1 and 0.3 BL/sec, showing an exponential decrease with age (size) which is linked to the increasing accessibility with age (size) to large forage biomass of deeper layers, thus decreasing the horizontal gradients of the feeding habitat index controlling the movement (Fig. 9).

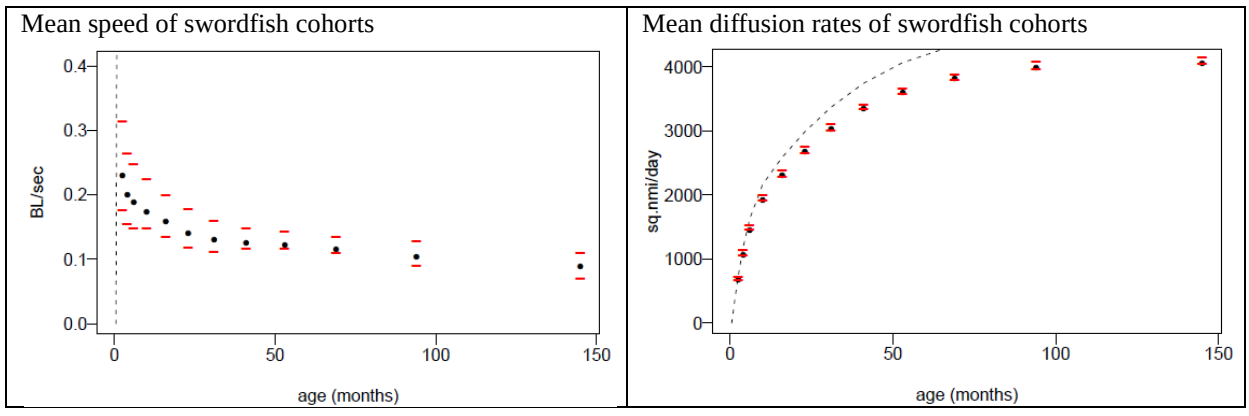

Figure 9: Maximum speed and diffusion rates by cohort (depending of age/size and habitat value / gradient) based on SEAPODYM parameterization (dotted lines) and predicted means weighted by the cohort density (black dots) with one standard error (red bars).

6. Biomass estimates and population dynamics

Three sub-stocks emerged from the simulation that represented very well the overall distribution of catch spatially, in the North Pacific, South-west Pacific and eastern Pacific (Figure 10). The spatial correlation between the adult swordfish density and the Japanese longline CPUE is remarkable (Fig. 10). There is a seasonal peak in density of adult fish associated to summer warming in the sub-temperate range of their habitat. Nevertheless, even in winter a large fraction of these fish inhabit these regions where they are fished all year round.

Spawning grounds and juveniles occur in tropical waters, and notably in the warm waters of the Kuroshio south of Japan from the end of summer to autumn. While growing immature fish concentrate in the tropical 20°N-20°S latitudes with a noticeable high density in the central eastern Pacific (Fig. 11), where the Korean longliners catch a significant number of immature swordfish. Both the distribution of observed catches and predicted density of young immature fish are strongly influenced by the El Nino Southern Oscillation (ENSO) with a large eastward spatial shift during El Nino events (Fig. 10).

The overall Pacific adult stock biomass was estimated between 3.7 -3.4 million tones (Fig. 13). This is certainly largely overestimated since i) the fishing mortality due to large fisheries in the EPO is not taken into account, ii) the diffusion parameter was estimated to its highest value thus increasing biomass everywhere in the model domain and iii) previous analyses with the model have shown a tendency to increase biomass to achieve a better fit to fishing data, especially when using coarse resolution (e.g. 2°x month) and when fisheries are defined (i.e., aggregated) with too much heterogeneity. Thus, it would be particularly useful to revise this study using higher resolution (eg. 1deg x month) environmental forcing and a complete fishing data set.

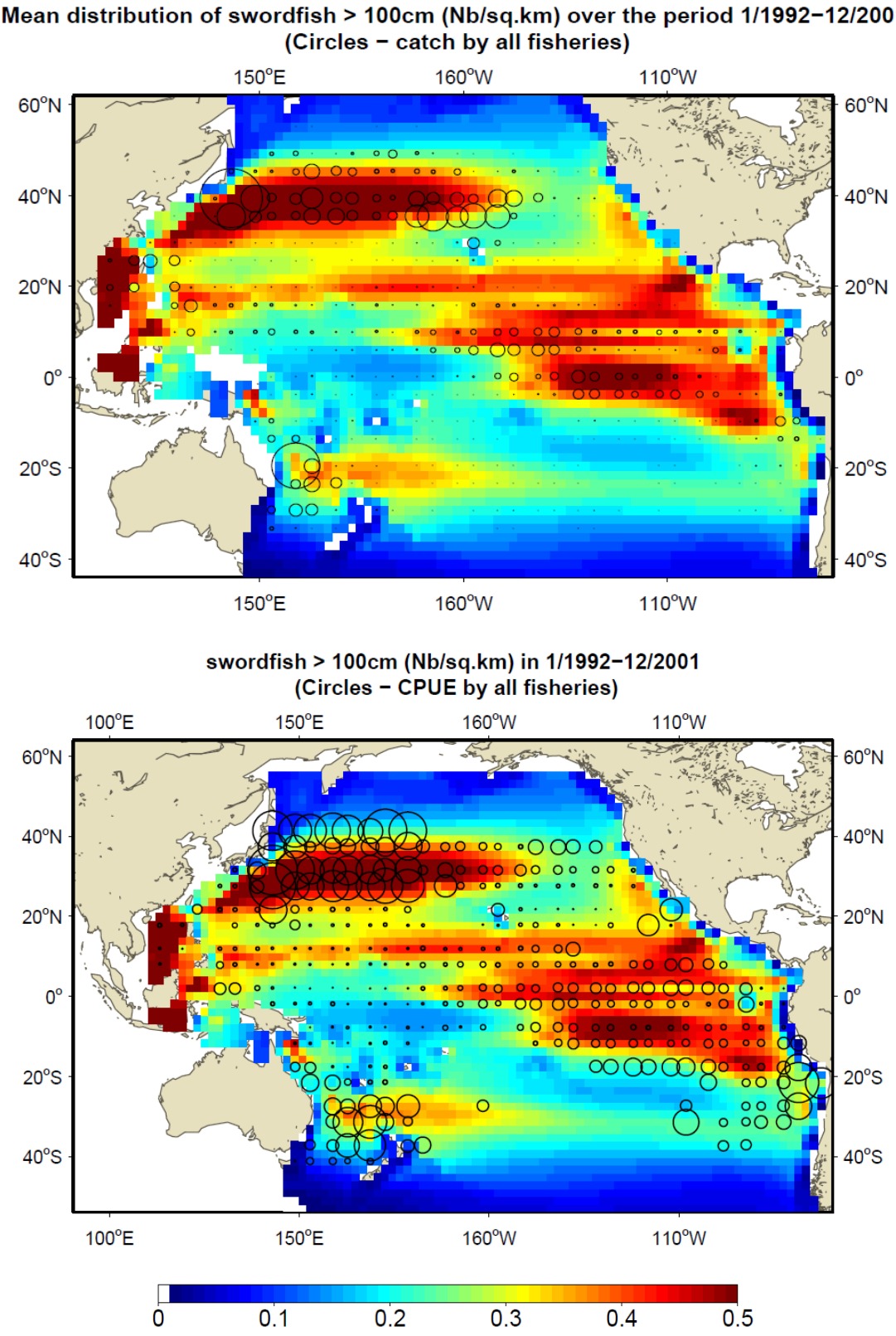

Figure 10. Mean distribution of swordfish larger than 100 cm (Nb / km^2) over the period 1992-2001 with Japanese fleet CPUE superimposed and proportional to the size of circles.

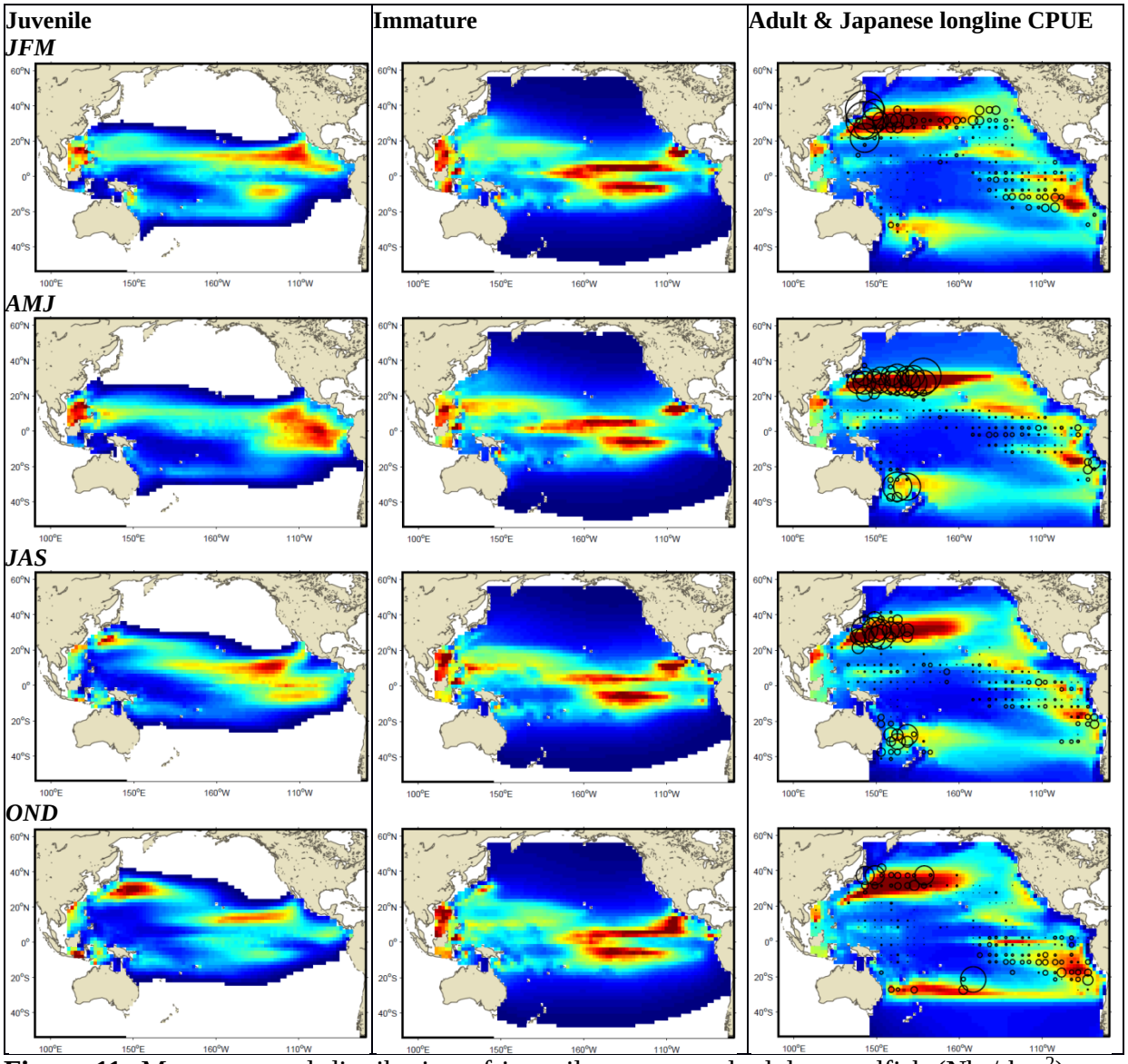

Figure 11: Mean seasonal distribution of juvenile, young and adult swordfish (Nb / km^2) over the period 1948-2003 with Japanese fleet CPUE superimposed and proportional to the size of circles. JFM stands for January-February-March, AMJ for April-May-June etc.

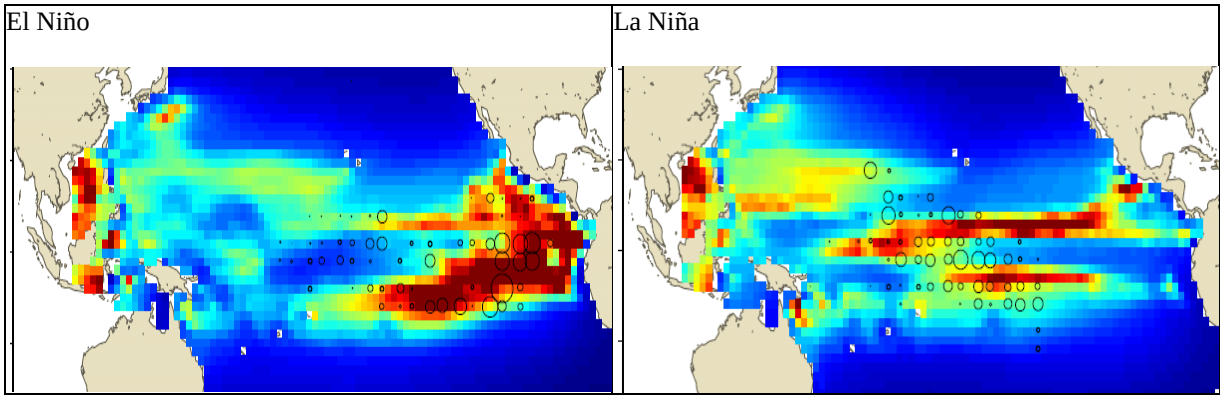

Figure 12. Distribution of young immature swordfish: distribution during El Niño and La Niña events with CPUE of Korean longline fishery.

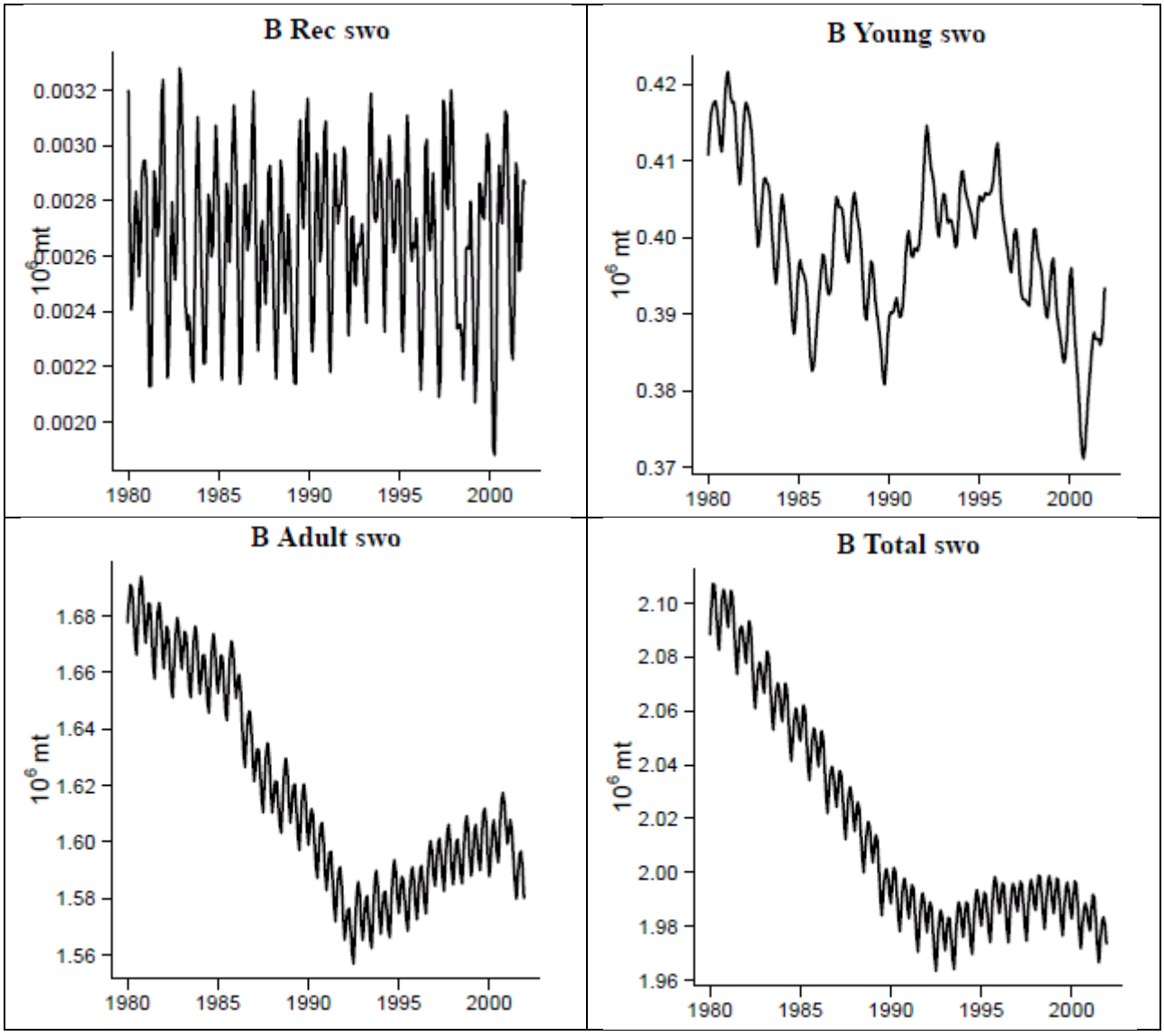

Figure 13. Total Pacific swordfish biomass estimates for recruits, immature, adult and all cohorts.

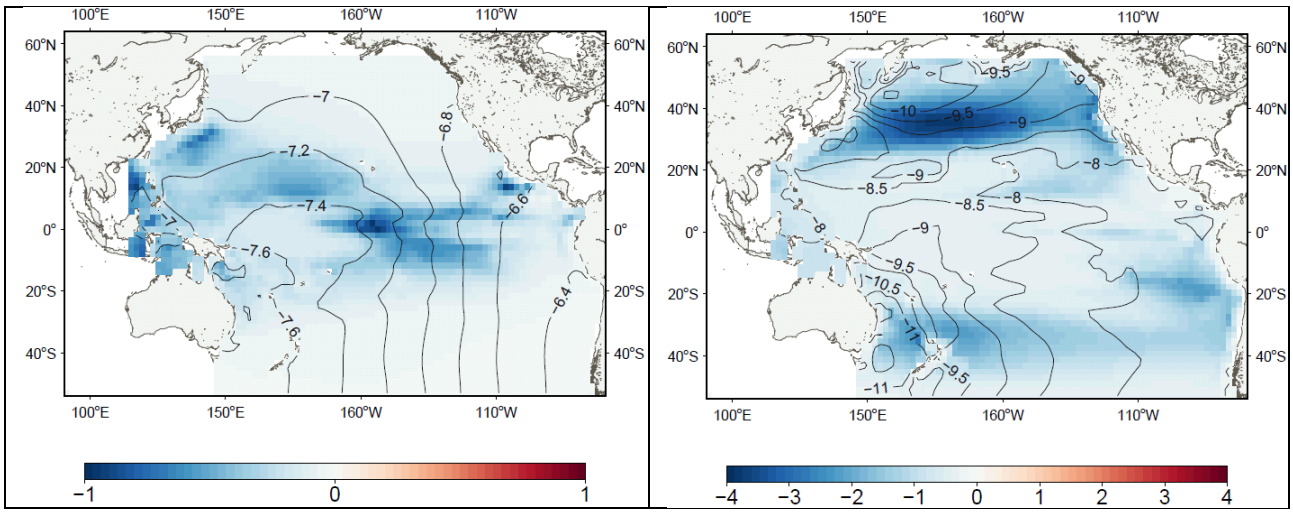

Figure 14. Spatial map showing the fishing impact quantification (color – dB = B-B(F0), contour lines – dB/B(F0)) for Pacific swordfish population given the estimated stock size: (left) immature cohorts, (right) mature population.